Materials Innovations

HΣXA Publishers

Dielectric Composites | Review Article | http://doi.org/10.54738/MI.2022.2202

# Materials Innovations in 2D-filler Reinforced Dielectric Polymer Composites

**Amjad Ali[1], Mirza Nadeem Ahmad[2], Tajamal Hussain[3]*, Ahmad Naveed[1], Tariq Aziz[4], Mobashar Hassan[1], Li Guo[1]***

**1** Research School of Polymeric Materials, School of Materials Science & Engineering, Jiangsu University, 212013, Zhenjiang, China
**2** Department of Applied Chemistry, Government College University Faisalabad, Faisalabad, Pakistan
**3** School of Chemistry, University of the Punjab, 54590, Lahore, Pakistan
**4** School of Engineering Yunqi Campus, Westlake University, Hnagzhou, 310024, Zhejiang, PR China.



**Received:** 13 January 2022
**Accepted:** 14 February 2022
**Published:** 27 February 2022

**Citation:** Ali A, Nadeem Ahmad M, Hussain T, Naveed A, Aziz T, Hassan M, Guo L (**2022**) Materials Innovations in 2D-filler Reinforced Dielectric Polymer Composites. *Materials Innovations 2* (2), 47-66.

***Correspondences**: (Tajamal Hussain) tajamalhussain.chem@pu.edu.pk (Li Guo) liguo@ujs.edu.cn



Published By Hexa Publishers

**ISSN**
Electronic: 2790-1963

*Polymer dielectric possess advantages of mechanical flexibility, low temperature processing, and cost. However, for practical applications dielectric constant of polymers is not high enough. To raise the dielectric constant, polymers are often composited with fillers of various morphologies (one-dimensional, two-dimensional, three-dimensional) and types (inorganic, organic, carbon, conductive, non-conductive). Recently discovered two-dimensional (2D) materials including graphene, transition metal dichalcogenides, MXenes, ferroelectric ceramics, etc. have been discovered. These materials have excellent electrical, mechanical, thermal properties and high specific surface area, which makes these ideal materials to reinforce the properties of polymers, especially dielectric properties. Here, in this review we summarize the latest developments regarding the use of 2D fillers to improve the dielectric properties of polymer composites. We have systematically discussed synthesis of 2D materials, processing of their 2D filler/polymer composites, theoretical background of dielectric properties of these composites, and literature summary of the dielectric properties of polymer composites with various type of 2D fillers.*

**Keywords:** Polymer composites, Dielectric properties, 2D fillers, Graphene

## INTRODUCTION

Among all the passive components (resistor, capacitors, and inductors), Capacitors call for special attention due to their applications in filtering, timing, A/D conversion, termination, decoupling, and energy storage materials. Dielectric materials are generally used for capacitor applications. Traditionally, inorganic materials have been used as the dielectric materials for energy conversion and storage. However, high temperature processing and mechanical brittleness have led to developments of alternate materials. Polymers are interesting dielectric materials due to their low temperature solution processing, low cast, large area processing, environmental stability, and mechanical flexibility. Due to these set of properties, 50% of market share belong to polymer based capacitors (Figure 1)[1]. Apart from electronic industry, high-k poly mer dielectrics have found many applications in civilian and military applications

including active vibration control, aerospace, underwater navigation and surveillance, hydrophones, biomedical imaging, non-destructive testing and air imaging microphones. High-k poly mer dielectrics have also been used as electromechanical devices to perform energy conversion between the electric and mechanical forms. These devices serve as artificial muscles, smart skins for drag reduction, actuators for active noise and vibration controls, and microfluidic systems for drug delivery and micro-reactors.[2−4]

One of the most commonly used dielectric polymers is polypropylene (PP), which has high breakdown strength ($E_b$) (>700 V/m), low dielectric loss (<0.02%), and temperature- and frequency-independent dielectric constant with good mechanical strength. However, it has a low dielectric constant (k = 2.2), impeding widespread applications.[5,6] Some high dielectric constant polymers such as PVDF and its co-polymers have been fabricated which possess dielectric constant as high as 50.[7] But still their dielectric constant is lower compared to dielectric ceramics. To improve the dielectric constant of polymers, fillers are successfully introduced into these polymers to raise their dielectric constants or electrical conductivity. These fillers include organic, metals, ceramics, and carbon based fillers.[8−20]

Recently, a new class of materials, i.e., two-dimensional (2D) materials have been discovered. 2D materials have fascinating mechanical, thermal, and electrical properties, which are suitable for variety of applications.[21−31] Examples of 2D materials Include graphene (Gr), transition metal dichalcogenides (TMDCs), Mxenes, boron nitride (h-BN), black phosphorous (BP), etc. Family of 2D materials is growing fast and thousands of 2D materials have been predicted theoretically, while hundreds can be synthesized experimentally. Due to their high surface area, these materials are also very useful for the polymer composite application as they can interface with polymers more effectively for improvement of mechanical, electrical, and thermal properties.[32,33] Recently, there has been a great interest in 2D-filler based polymer dielectric composites.[34−36] In this review, we will summarize the latest developments related to use of 2D materials for polymer composites for dielectric applications.

## SYNTHESIS OF 2D MATERIALS

2D materials can be synthesized by mechanical exfoliation, chemical vapor deposition (CVD), and wet chemical synthesis. Mechanical exfoliation is not scalable hence not suitable for the polymer composites. CVD growth was initially use for electronics applications, but recently, significant developments have been made for large scale growth and transfer of CVD growth, which render CVD grown 2D materials suitable for polymer composite applications.[37] Perhaps, the best 2D materials growth route for polymer composites application is wet chemistry, which can produce ton scale 2D materials at a low cost. However, quality of materials grown with wet chemistry is inferior to CVD grown materials. Below, we will summarize the synthesis techniques of 2D materials for the polymer composites applications.

### Liquid phase synthesis

Liquid phase synthesis can be further divided into categories such as simple exfoliation, intercalation exfoliation and functionalization based exfoliation of 2D materials from bulk layered materials. Bulk layered materials have week van der Waals forces between layers, hence layered materials can be simply exfoliated by using external mechanical forces such as ultra-sonication in suitable solvent. A suitable solvent should have a matching surface tension with the solvent material. For example, exfoliation of graphite needs a solvent with surface tension of 40 $mJ/m^2$.[38] However, surface tension values can be fine-tuned using surfactants or/and by adding other solvents.[39,40] Variety of 2D materials including molybdenum sulfide ($MoS_2$), boron nitride (BN), tungsten sulfide ($WS_2$), tin sulfide (SnS), black phosphorous (BP), molybdenum selenide ($MoSe_2$), etc., in various solvents such as N-methyl-pyrrolidone (NMP), acetone, N, N-dimethylformamide (DMF), N-vinyl-pyrrolidinone (NVP), isopropanol (IPA), and dimethylsulphoxide (DMSO).[31,38,41,42] For example, shear mixing/ultra-sonication of graphite in NMP yielded high quality Gr with $I_D/I_G$ ratio between 0.1 to 0.4.[38,43] There are certain advantages and disadvantages of using exfoliation techniques for 2D materials synthesis. Exfoliation produces materials with fewer defects, however, yield of monolayer is low. Moreover, absence of any functional groups on exfoliated 2D materials lead to poor interaction between polymer and 2D materials. Size of exfoliated 2D sheets can vary with force. Sheer mixing produce sheets with size in few micrometers, while ultra-sonication produces sheets with size less than 1 micrometer. Liquid exfoliation can be improved with oxidation/functionalization of 2D materials, but can impart significant defects to basal plane of 2D materials. For example, strong oxidizing agents such as $KMnO_4/KClO_4$ and $H_2SO_4/HNO_3$, are used to oxidize the graphite surface, this oxidized graphite then can be dispersed in polar solvents to exfoliate graphite into Gr sheets (Hummer method)[44]. Sonication may be further required to facilitate the exfoliation of Gr in the polar solvents. Other 2D materials such as BN, $MoS_2$, $WS_2$ have also been synthesized by using this method or its modifications.[45,46] A large sheet size can be obtained using this method, which leads to formation of liquid crystal.

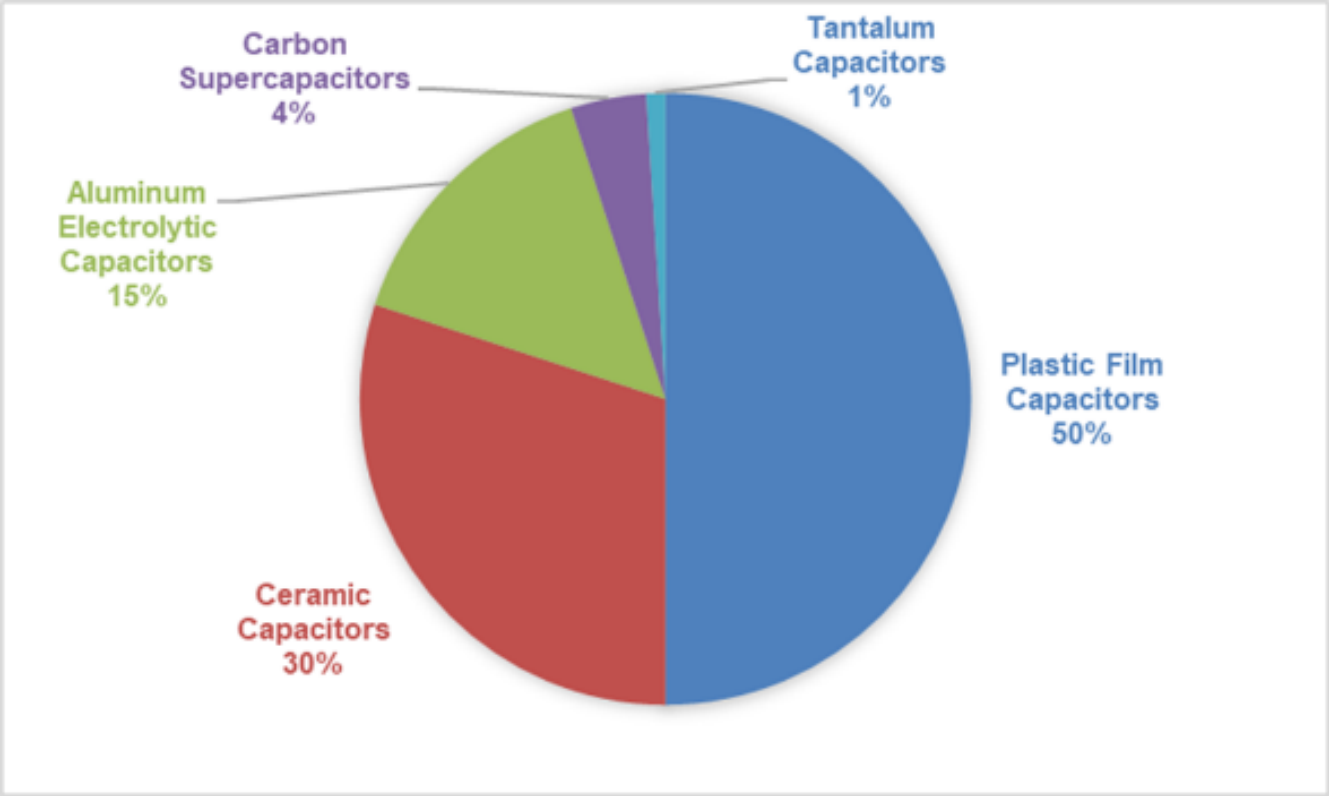


*Figure 1. Market share of different materials based capacitors.*[1]

Another way to achieve the exfoliation at milder conditions, intercalation of the layered material is a preferred route. For example, lithium intercalation is widely used for exfoliation of $MoS_2$. A typical procedure involves immersing the bulk $MoS_2$ in n-butyl lithium (n-BuLi)/hexane solution for few days, which help intercalates the lithium ions between the layers of $MoS_2$.[47] This intercalated compound is subsequently transferred to the water, where production of gaseous products helps exfoliate the $MoS_2$. This process can be improved by modifying the procedure and changing the chemical reagents. For example, electrochemical intercalation process can also be employed to obtain Li intercalated compounds, which significantly reduce the intercalation time for days to hours.[48,49] Similarly, solvothermal reaction was exploited for intercalation of n-BuLi at 100 °C in bulk $TaS_2$. Due to energy provided by high temperature, the intercalation of Li+ was achieved in much shorter time (2 h).[50] Monolayer of TaS2 was obtained with mere mechanical shaking of lithinated bulk $TaS_2$ Figure 3(a & b). Other 2D materials such as $WS_2$[51], $MoSe_2$[52] have also been obtained by using this method. However, this method has certain disadvantages. For example, 2D materials obtained through this method are metallic and extra heating step is required to restore the semiconducting properties of obtained 2D materials. Moreover, Li is a flammable material and monolayer yield is also low.

## CVD Synthesis of 2D materials

Compared to liquid exfoliation, CVD is a bottom up synthesis methods. In a typical CVD method, a metal substrate is exposed to a volatile precursor, which decomposes/reacts on the metal surface to produce a 2D materials. Various metal substrates including Cu, Ni, $SiO_2$ have been used. Choiceof the precursor (metallic or non-metallic) depends on the final composition of the 2D material. Using CVD, elementary, binary, tertiary or even quaternary and quinary compounds have been fabricated. Gas flow, temperature and precursors controls the quality of the 2D materials. Summary of key parameters for CVD growth of 2D materials is described in Figure 4. Recently, Zhou et al.[53] have demonstrated a molten-salt-assisted CVD method which can be applied for the synthesis of a wide variety of 2D (atomically thin) materials. Crystal size and quality of the materials can be easily controlled by flow of metal (Figure 4). They successfully

demonstrated the synthesis of 47 compounds (including 32 binary, 11 ternary, one quaternary, one quinary, and two heterostructured compounds), see Figure 6. While CVD growth can produce variety of 2D materials with high quality, however, this method is

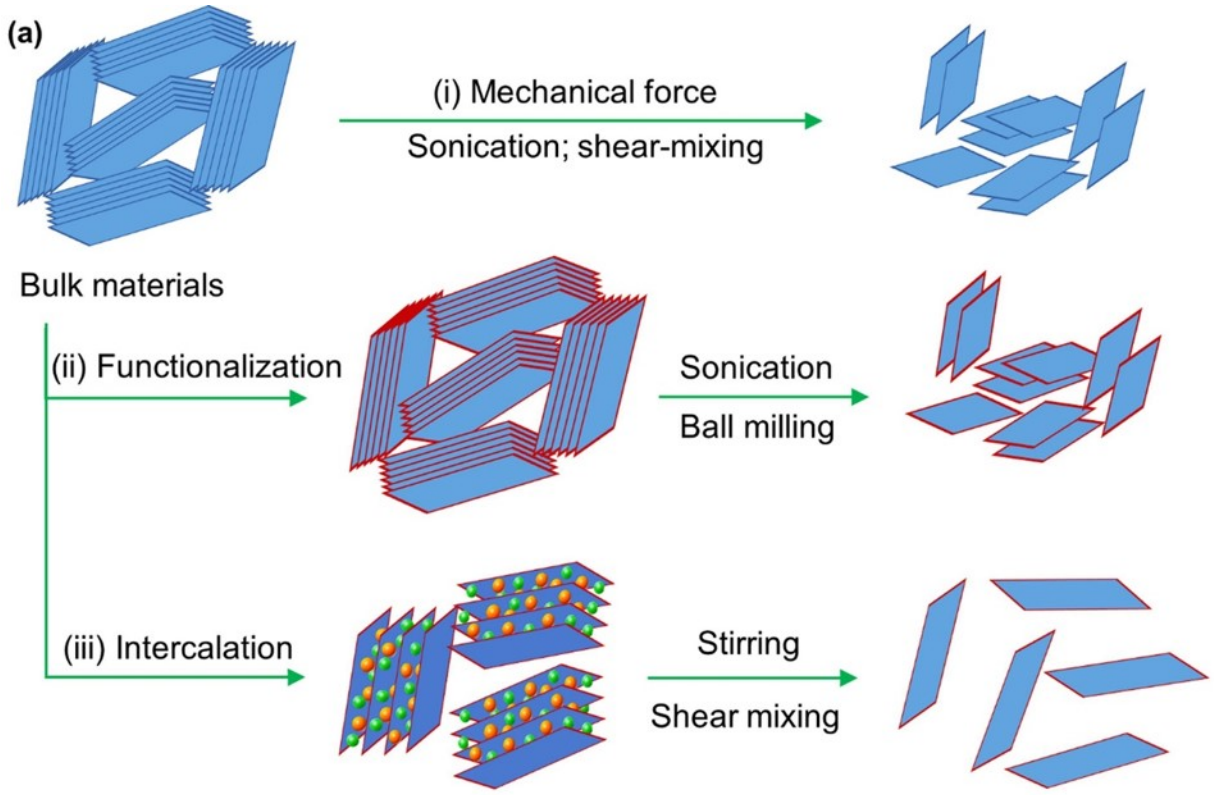


*Figure 2. (a) Schematics showing three types of solvent-based exfoliation techniques.*[35] *Reproduced with permission from ref. 35. Copyright (2021) Elsevier.*

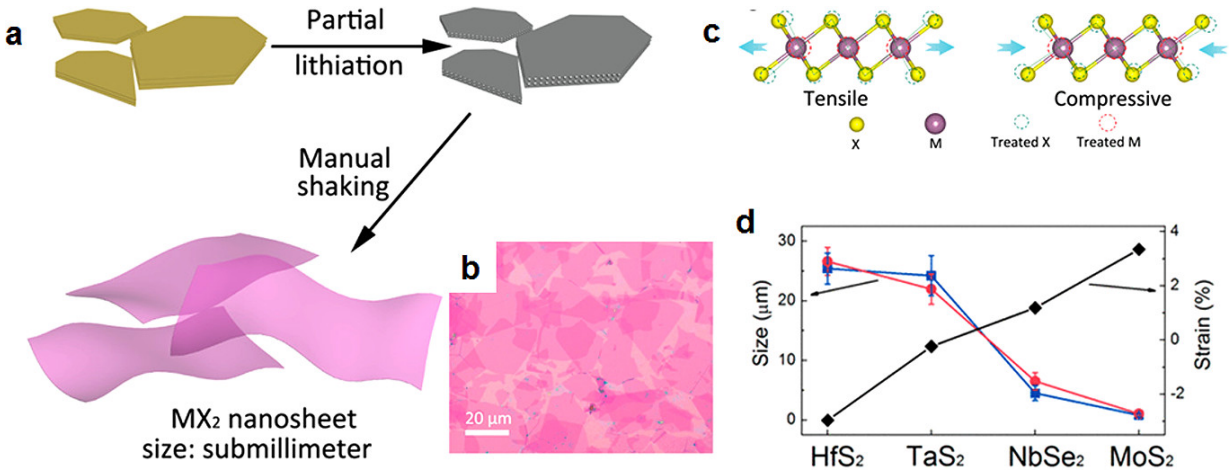


*Figure 3. (a) Schematic illustration for the manual shaking exfoliation process of partiallylithiated $Li_xMX_2$ into single layers. (b) Optical microscopy image of exfoliated single-layer $TaS_2$ nanosheets on a $SiO_2$/Si substrate.*[50] *Reproduced with permission from ref. 50. Copyright (2017) American Chemical Society.*

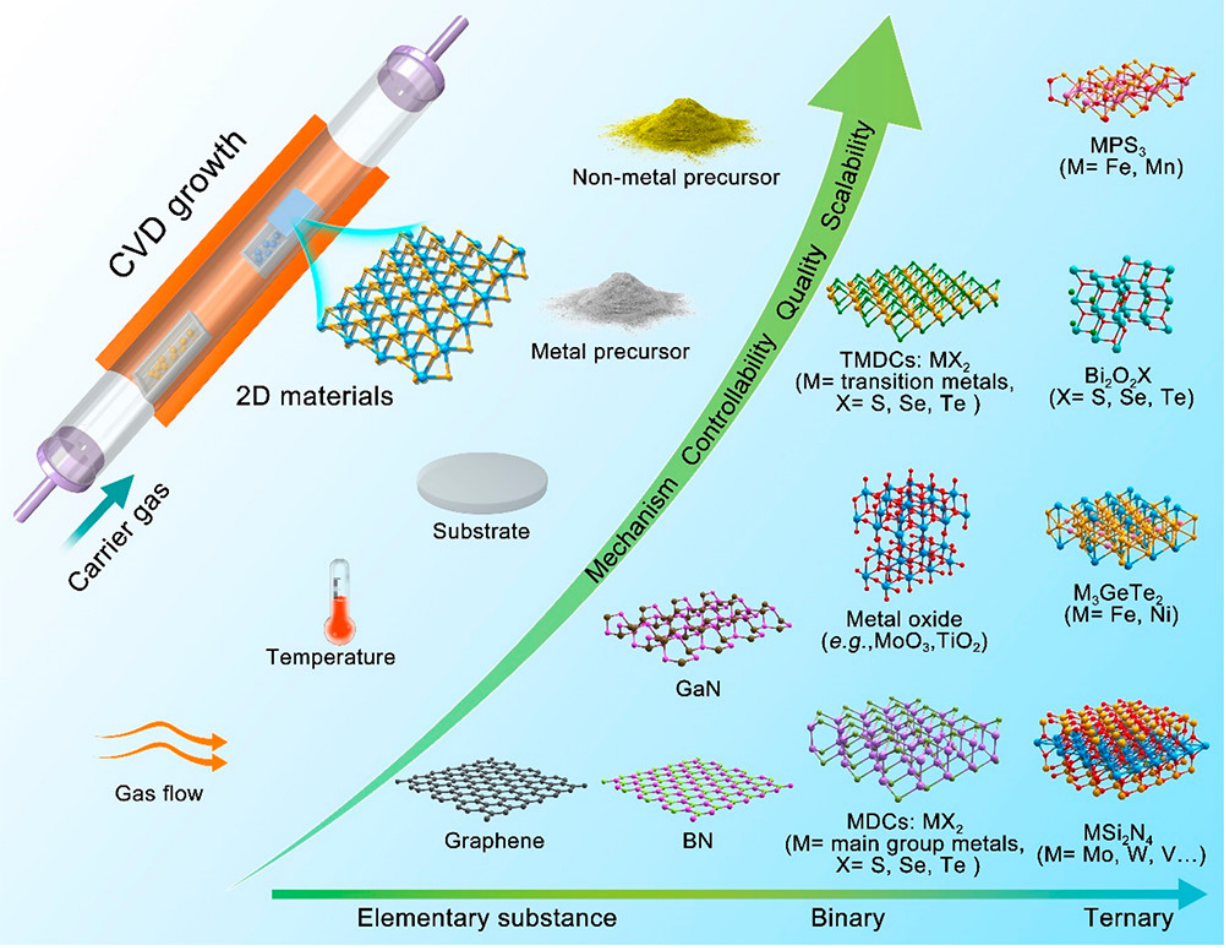


*Figure 4. Schematic of the key parameters for the CVD growth of 2D materials ranging from elementary substance, binary, and ternary to complicated materials.*[54] *Reproduced with permission from ref. 54. Copyright (2020) American Chemical Society.*

not scalable for all the 2D materials. Only handful of 2D materials can be produced on large scale. Apart from large scale production, large scale automatic transfer of CVD grown 2D materials is also another issue. CVD grown materials need to be transferred from growth substrate to desired substrate which involves exposure to chemicals, which can induce lot of impurities during the process. For Gr, roll-to-roll, and batch–to–batch industrial scale production has already been demonstrated. Also scalable transfer methods have been implemented for Gr.[37] However, for other 2D materials, large scale production and transfer is still a challenge.

## PROCESSING OF 2D-FILLER/POLYMER COMPOSITES

Polymers can be mixed with 2D materials with direct compounding, melt compounding, solution mixing or in-situ polymerization. Direct compounding involved direct missing of both solids (polymer and filler) and subsequently hot pressed to obtain final composites. This method is easy but dispersion and homogeneity of the mixture may not be ideal and is seldom used. In melt processing, polymers are melt above or close to their melting temperature and fillers are mixed. Due to high viscosity of polymers, a large sager force is required to disperse the filler properly in the polymer matrix. Twin screw extruders due to their good dispersive/distributive missing capabilities is the most popular equipment for dispersing and processing the polymer composites.[55] In this technique, under large shear force, fillers get aligned. Zhang et al. fabricated high density polyethylene (HDPE)/BN composites by mixing their different ratios and compounding in corotating twin screw extruder, cut into small pieces and dried, and were subsequently extruded by the multistage stretching extrusion BN sheets were aligned in the extrusion direction with anisotropy index of 480%.[56] For low viscosity polymers, technique such as mechanical or magnetic stirring might also work.

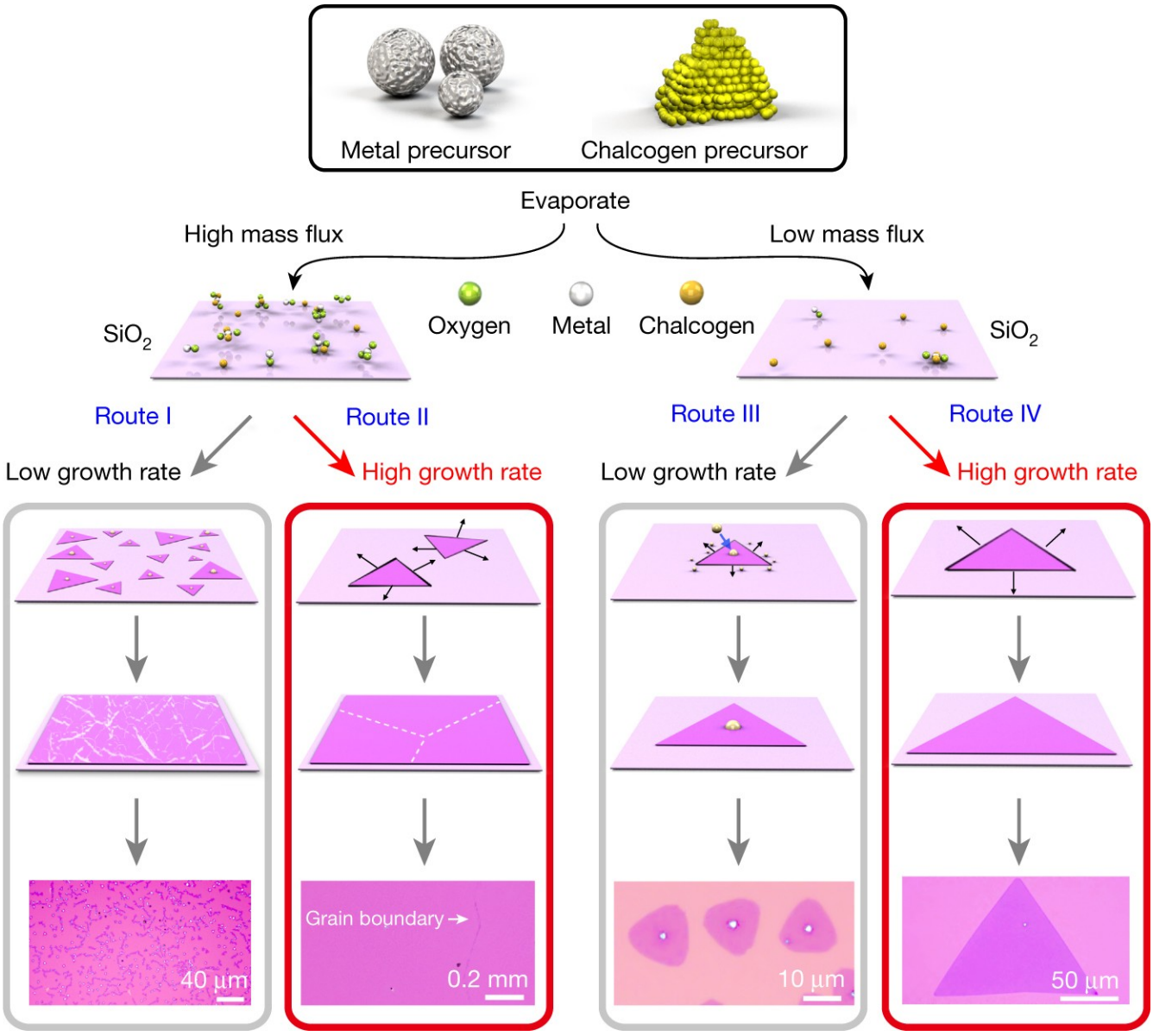


*Figure 5. Four different growth routes of 2D TMCs. Route 1 produces monolayer polycrystalline films with smaller grain size. Route II produces monolayer polycrystalline films with large grain size. Route III produces discrete monolayers with smaller crystal size. Route IV leads tomonocrystals with large size.*[53] *Reproduced with permission from ref. 53. Copyright (2018) Nature Publishing Group.*

Liquid phase processing of composites, including solution mixing and in-situ polymerization, is the most commonly used techniques. In solution based mixing, polymer is first dissolved in a solvent and then fillers are introduced with constant stirring. Sonication is often used to disperse the filler in the polymer, however, prolonged sonication can introduce the damage to filler. If the viscosity of the liquid is too low, fillers tend to agglomerate, once the stirring/sonication is stopped. For better dispersion fillers can be modified with different functional groups. In in-situ polymerization, fillers are introduced in the monomer solution. Then monomer is polymerized under constant stirring. This method is associated with better filler dispersion in the polymer matrix due to the better interaction with polymer and filler. To improve/control the filler distribution, dispersion and alignment, various strategies such as (i) the self-assembly based on the LC phase formation in aqueous solutions or liquid polymers; (ii) the forced assembly driven by external forces (tap casting, wet spinning, vacuum assisted

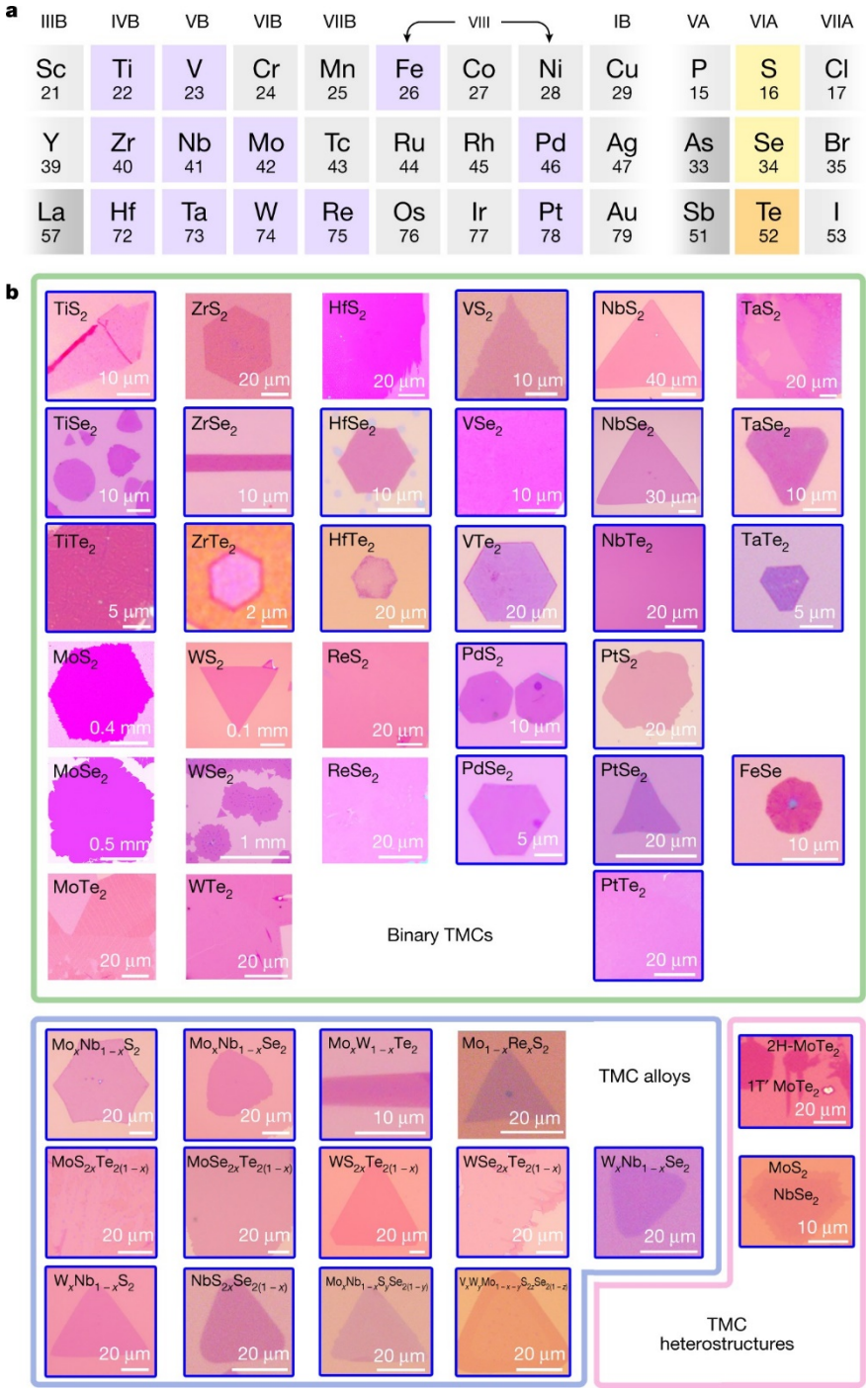


*Figure 6. (a) Overview of metals (highlighted in purple) andchalcogens (highlighted in yellow and orange) that can form layered sulfides, selenides and tellurides. (b) Optical images of 47 TMCs synthesized using our method. TMCs that have not been previously synthesized are outlined in blue.*[53] *Reproduced with permission from ref. 50. Copyright (2018) Nature Publishing Group.*

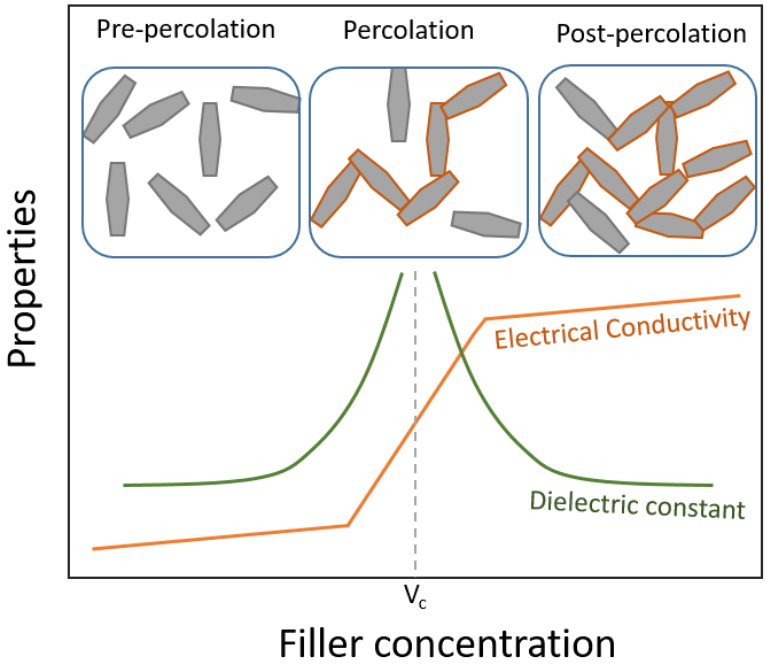


*Figure 7. Schematics showing changes in physical properties in the pre-percolation, percolation, and post-percolation region. Note the rapid change in electrical conductivity and dielectric constant in the vicinity of percolation threshold ($V_c$).*

filtration, electric field based alignment, magnetic field based alignment, electrophoretic dispersion) and (iii) the assembly directed by well-defined templates (unidirectional freeze casting, bidirectional freeze casting, using 2D and 3D templates) have been employed. Details of these methods can be found elsewhere.

## THEORETICAL BACKGROUND ON DIELECTRIC PROPERTIES OF COMPOSITES

For conductive filler, electrical conductivity and dielectric constant can be predicted by percolation threshold. At the filler concentrations lower than a particular filler concentration (pre-percolation), fillers are dispersed in isolation from each other, though some local network exist. At pre-percolation, the electrical conductivity and dielectric properties show negligible effect with the filler concentration. When filler concentration reaches a critical concentration ($V_c$), global networks start to form in the polymer matrix (percolation threshold) and electrical conductivity and dielectric constant see a sharp increase. After percolation threshold, electrical conductivity saturates against the filler concentration and dielectric constant drops sharply.[9,14,55]

At percolation threshold electrical conductivity and dielectric constant can be expressed as

$$k \propto (V - V_c)^{-s}$$

$$\sigma \propto (V - V_c)^{t}$$

Where k is the dielectric constant, V is the filler concentration, $V_c$ is the filler concentration at percolation threshold, s and t are critical constants. Value of t is between 1.6-2 for a 3D system and value of s is between 0.8-1.[9,14] However, these values are not always observed in practical system.

Percolation threshold for 2D fillers can is given by following equation,

$$V_c = \frac{2\pi D^2 t}{4(D+D_{IP})^3}$$

Where $D_{IP}$ is distance between two filler platelets, D is the diameter of the 2D fillers and t is the thickness. In practical, this equation is seldom obeyed, as fillers tend to agglomerate in the polymer matrix.

For non-conductive fillers, the dielectric constant of the composites can be given by the Maxwell-Garnett equation below[57],

$$k_c = k_m \left(1 + \frac{V\,(k_f - k_m)}{A\,(1-V)(k_f - k_m) + k_m}\right] \times \pi r^2$$

Where kc, km, and kf are the dielectric constants of the composite, filler and the matrix, composites, respectively. Value of A=1/3. This equation is only valid for the low concentration of fillers, for high filler concentration system, Jaysundere–Smithe quation can be employed, which accommodates inter-filler forces at higher filler concentrations. Lichtenker and Bruggeman equa-

tions are also applied in some cases to predict the dielectric constant of non-conductive filler based polymer composites.[58,59]

## DIELECTRIC PROPERTIES OF 2D FILLERS/POLYMER COMPOSITES

### Dielectric properties of conductive 2D-filler/polymer composites

Conductive 2D fillers mainly include MXenes and Gr based materials. 2D Gr fillers can be fabricated as pristine Gr, graphene oxide (GO) or reduced graphene oxide (rGO). Pristine Gr has good crystal structure and hence excellent electrical, which can be imparted to polymer matrix to fabricate the dielectric polymer composites. Close to the percolation threshold Gr sheets form a miacrocapacitor like structures in polymer matrix and due to Maxwell-Wagner-Sillar (MWS) polarization, hence, dielectric constant of the composites increases significantly. Li et al. added graphite nanoplatelets (GNP) to polyvinylidene fluoride (PVDF) matrix to fabricate dielectric composites. Percolation threshold at a low GNP filler concentration of 2.4 wt. % was obtained, as shown in Figure 8a. Near percolation threshold at 1KHz frequency, dielectric constant of 173 and a low loss tangent value of 0.65 was obtained.[60] As typical of percolative composites, near percolation threshold, conductivity increase significantly with the frequency, while dielectric constant decreases at high frequencies, as shown in Figure 8(a-c). Similarly, Chu et al. reported few layer graphene (FLG) nanosheet/PVDF sandwich composites with dielectric constant as high as $10^5$.[61] Though pristine Gr has good electrical properties, it doesn't have dangling bonds, hence, its dispersion in polymer matrix is difficult, which can effect reproducibility of the dielectric properties of the polymer composites, and also lead to poor mechanical properties. For better dispersion in the polmyer matrix, pristine Gr was modified with Ionic liquid (GIL) before mixing with PVDF matrix. Percolation threshold of GIL/PVDF composites was 1.86 vol.% and of Gr/PVDF composites was 0.67 vol.%. Compared to Gr/PVDF composites, dielectric constant of GIL/PVDF composites was recorded higher (167 compared to 90 for Gr/PVDF composites) due to MWS polarization at GIL and PVDF interface.[62] Wang et al. produced hydroxyl-modified graphite micro-sheet and mixed those with PVDF matrix. Dielectric constant value of $6.5 \times 10^5$ at test frequency of 100 Hz was obtained at 6 wt.% of fillers. They also obtained a high breakdown strength ($E_b$) of 0.63 kV/mm and specific energy storage value of 2.07 J/cm$^3$.[63] Gr have also been modified with polymers such as polyvinyl pyrrolidone (PVP), polyaniline (PANI), etc., for better dispersion into polymer matrix.[64] Lv et al. modified graphene nanoparticles (GNPs) with PANI through in-situ polymerization of PANI and obtained GNPs@PANI to subsequently mix with oxidized styrene-butadienestyrene copolymer (SBS-FH), see Figure 9.[65] GNPs@PANI showed better dispersion in SBS-FH matrix compared to GNPs, as former had a better interaction with polymer due to the diploe-dipole and hydrogen bonding interaction. Since the PANI was dedoped, its coating on GNPs resulted in blockage of direct contact between conductive GNP fillers, which greatly enhances the MWS polarization, which subsequently give rise to large dielectric constant values. Value of percolation threshold and highest possible dielectric constant for GNPs/SBS-FH and GNPs@PANI/SBS-FH was 1.19 vol.% and 9.38 vol.%, and 15.96 and 56.8 @ 1000 Hz, respectively, see Figure 10.

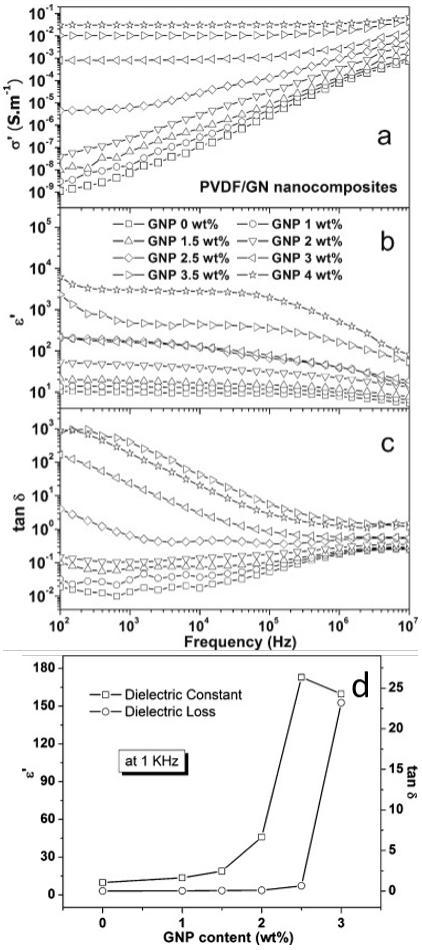


*Figure 8. (a) Frequency vs conductivity, (b) frequency vs dielectric constant, and (c) frequency vs loss tangent of GNP/PVDF composites. (d) Dielectric properties of the GNP/PVDF composites against filler concentration at 1 KHz frequency.[60] Reproduced with permission from ref. 60. Copyright (2010) Elsevier.*

Most commonly used Gr is fabricated in the form of GO, where Gr is oxidized with Gr. Presence of oxygen functional groups not only help Go disperses well in the polymer matrix but also open the pathways for further functionalization of the Gr with other materials. Moreover, as mentioned above, low conductivity contact filler contact between GNPs@PANI particle can enhance the dielectric constant, similar result may be obtained for GO, as it has low conductivity compared to pristine Gr. He et al. has prepared

GO/PVDF composites with percolation threshold as low as 1 vol.% and dielectric constant as high as $10^7$was obtained.[66] GO has been further modified with other materials such as PVP[67], ionic liquid amine, polyvinyl alcohol (PVA)[68], phosphorus salt[69], and p-Phenylenediamine (PPD)[70] to mix with polymer matrix for better dispersion and improved dielectric properties.

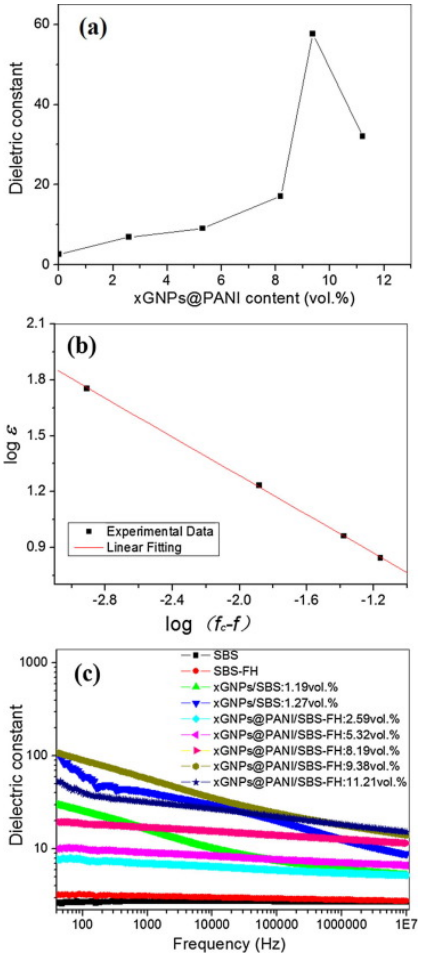


*Figure 10. (a) Dielectric constants of xGNPs@PANI/SBS-FH composites as a function of filler content at 1000 Hz. (b) Percolation threshold calculation. (c) Dielectric constant as a function of frequency at different filler contents.*[65] *Reproduced with permission from ref. 65. Copyright (2018) Elsevier.*

Between two extremes of Gr, i.e., pristine Gr and GO, reduced GO (rGO) is a better choice as a filler as it has enough functional groups to aid the better dispersion of Gr in polymer matrix and also retains most of the excellent electrical properties of pristine Gr. Yuan et al. fabricated rGO/PDMS composites with dielectric constant value of 753 at the percolation threshold, which is 260 times higher than that of pure PDMS.[71] Liu et al. demonstrated that dielectric constant of rGO based composites may be lower than Gr based composites, however, dielectric constant increase significantly for GO composites with increases reduction. For rGO with C/O ratio of 2.79 dielectric constant of polyimide (PI) composites was 10, while for rGO with C/O ratio of 2.96 dielectric was about 60, clearly indicating dielectric constant increased with degree of reduction.[72] Due to use of different polymer matrix and differently prepared Gr, GO, rGO and functionalized Gr, it is impossible to directly compare the effect of change in Gr structure on dielectric properties from different literature sources. In an attempt to systematcailly investigate the effect of Gr structure on dielectric properties of composites, Li et al.[73] produced five graphene derivatives, namely, GO, rGO, electrochemical exfoliated graphene (EG), and 3,4,9,10-perylenetetracarboxylic acid (Py)-modified rGO (PyrGO) and EG (PyEG) (Figure 11), and studies their effect on the dielectric properties of PVDF composites.[73] Amongst all the compoistes, PyEG/PVDF composites showed best dielectric constant (Figure 12). At percolation threshold, PyEG (0.74 vol%)/PVDF composites exhibited a dielectric constant of 480 at 1 kHz, with a relatively low dielectric loss of 0.27. GO had lower conductivity, rGO and PyrGO had relatively better conductivity than GO but lower dispersion, EG had good conductivity but poor dispersion, PyEG had good dispersion due to presence of Py and also had good electrical properties due to pristine structure of EG as interaction between Py and EG is non-covalent. Hence, PyEG had best dielectric properties.

MXenes are other members of 2D family, which have conducting properties. Initially, explored for energy storage applications, MXenes have slowly found their applications for polymer composites due to their excellent electrical properties. Tiu et al. have reported $Ti_3C_2T_x$/poly(vinylidene fluoridetrifluoro-ethylene-chlorofluoroehylene) (P[VDF-TrFE-CFE]) with dielectric constant as high as $10^6$ at 1HZ frequency at relatively high percolation threshold of 15.3 wt.% of MXene due to the relatively low average lateral sheet size of 4.5 $\mu$m. The percolation threshold further increased to 16.8 wt.% when the size further reduced to 1.5 $\mu$m and dielectric constant reduced to 9120.[74] It must be mentioned here that Gr sheets have relatively large size and hence need relatively low filler concentration to achieve percolation threshold compared to MXenes. GNPs with large lateral sizes of 25 $\mu$m delivered a giant k value of over $10^7$ at a much lower filler loading of 2.3 vol% than the $Ti_3C_2T_x$ nanosheets.[75] However, it must be noted that 2D fillers, anyways, are better than 0D, 1D and 3D fillers.

In addition to single phase 2D conductive fillers, 0D, 1D filler and other conductive and non-conductive fillers can also be added to polymer to fabricate multiphase polymer composites. Example of such composites are carbon nanotubes/GNP/Thermoplastic urethane (TPU)[76], Gr/PDA@Ag/TPU[77], BT/$Ti_2C_3T_x$/PVDF[78], $\alpha$-SiC/$Ti_2C_3T$/PVDF[79] where a third phase is added to binary system to improve the dielectric properties.

## Dielectric properties of non-conductive 2D-filler/polymer composites

While conductive filler based percolative composites can achieve high dielectric constant at low filler concentration, dielectric loss of such composites is usually high. Alternate strategy to improve the dielectric composites

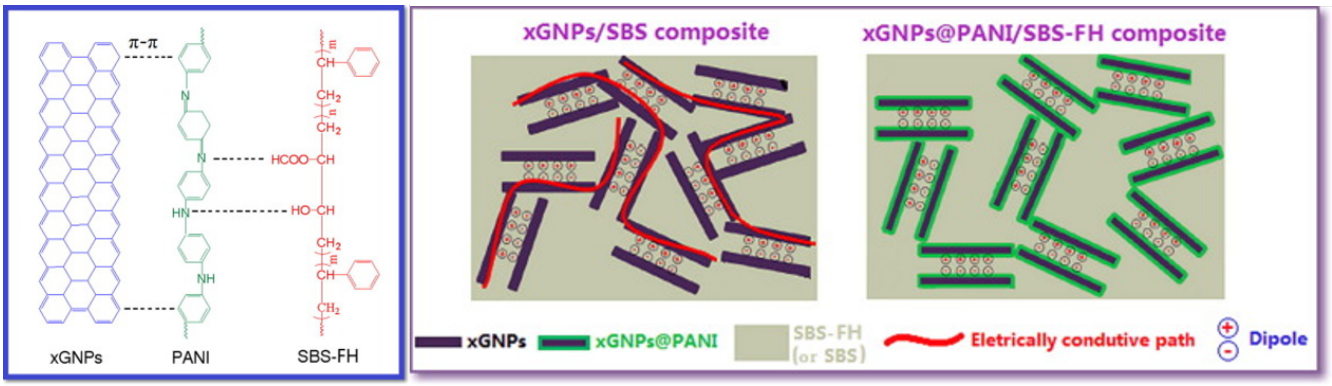


*Figure 9. Functionalization scheme of GNPs and dispersion of GNPs and modified GNPs in polymer matrix.*[65] *Reproduced with permission from ref. 65. Copyright (2018) Elsevier.*

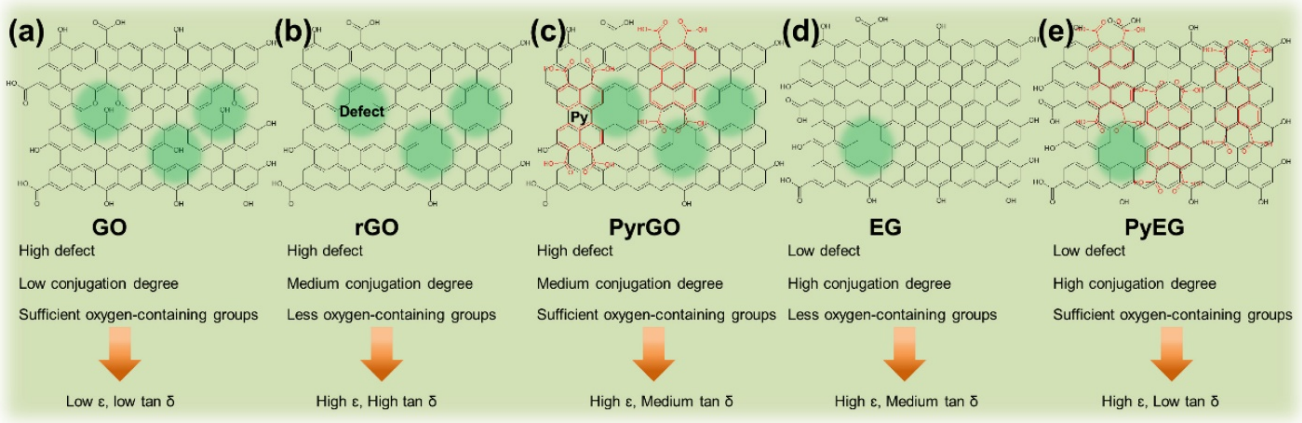


*Figure 11. The structure illustration and characteristics of (a) GO, (b) rGO, (c) PyrGO, (d) EG and (e) PyEG and corresponding dielectric behaviors of their PVDF composites.*[73] *Reproduced with permission from ref. 73. Copyright (2019) Elsevier.*

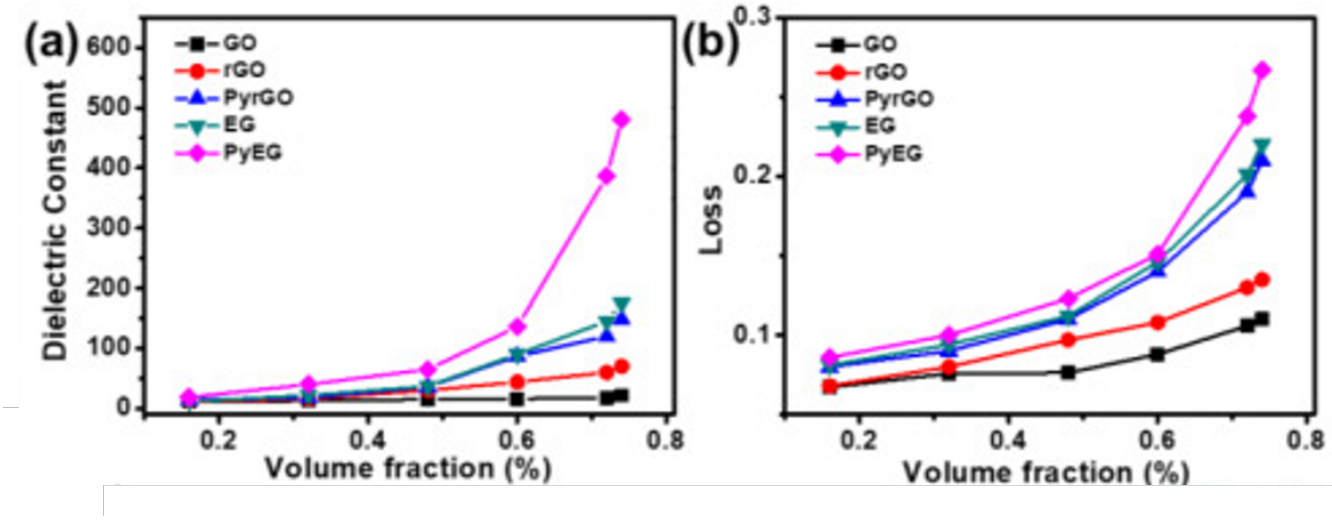


*Figure 12. The dielectric constants and (b) losses of GO/PVDF,rGO/PVDF, PyrGO/PVDF, EG/PVDF and PyEG/PVDF composites with different filler contents.*[73] *Reproduced with permission from ref. 73. Copyright (2019) Elsevier.*

is to add insulating 2D fillers. Compared to conductive filler, addition of non-conductive fillers will moderately increase the dielectric consant but then dielectric loss is low, which results into high $E_b$ and high energy density ($U_d$). Boron nitride (BN) is a representative 2D non-conductive filler. BN is a wide band gap filer with Eb of 800mV/m. BN nanosheets have been mixed with various polymer matrices including chitin[80], poly(vinylidene fluoridechlorotrifluoroethylene) (P[VDF-CTFE])[81], PMMA[82], poly(aryl ether sulfone)[83], etc. With addition of BN nanosheets, $E_b$ of Chitin and P[VDF-CTFE] was increased by 40% and 85%, respectively.[80,81] Similarly, with addition of BN, greater energy density at good $E_b$ has been reported for polymer composites. BN/PMMA composites at 10 wt.% BN laoding exhibited $U_d$ of 3.5 J/cm$^3$ at 400 MV/m, with an efficiency of 86%.[82] BN/ poly(aryl ether sulfone) Ud of 4.2 J/cm$^3$ at 500 MV/m ,with an efficiency of 86%.[83] Similarly, BN/divinyltetramethyldisiloxane-bis(benzocyclobutene) (c-BCB) composites exhibited $U_d$ of 1.8 J/cm$^3$ and an efficiency of about 70% at 403 MV/m. In addition to excellent dielectric properties, BN based polymer composites also show good temperature stability of dielectric properties. Mica is another insulating 2D material which can be added to polymers to reinforce their dielectric proeprties. Upon addition of Ultra-sonic exfoliated mica sheets were to PMMA grafted terpolymer (P(VDF-TrFE-CTFE)-g-PMMA), discharging efficiency of the composites reached ~78% under 250 MV/m. The $U_d$ of the optimized composite reaches 9.6 J/cm$^3$, which is nearly 290% that of the pristine terpolymer.[84] 2D metal oxides and hydroxide have also been used as fillers for improvement of polymer dielectric properties. Ji et al.[85] studied $Ni(OH)_2$ morphological and dielectric properties of $Ni(OH)_2$ nanoplatelets and flowers based PVDF composites. Composites showed 300% enhancement in $U_d$. Suchenhancement was result of linkages between filler and PVDF due to presence of OH groups on filler, high specific surface area of filler which lead to enactment of $\beta$-phase polarization, and less concentrated electric filed due to high anisotropy of fillers in the matrix.[85] 2D $ZrO_2$[86] and $Al_2O_3$[87] fillershave also been introduced to the polymer matrix to improve dielectric properties. While exploring effect of $Al_2O_3$ on c-BCB, Li et al.[87] also demonstrated superior efficiency of 2D nanoplatelets (NPLS) compared to 0D nanoparticles (NPs)and 1D nanowires (NWs) of $Al_2O_3$ in enhancing dielectric properties. Authors demonstrated that compared to 0D particles and 1D nanotubes, 2D NPLS of $Al_2O_3$ is most effective in uniformly dispersing the applied electric field (Figure 13a) and in hindering the growth of breakdown phase under high external electric fields and elevated temperatures (Figure 13b), which results in highest $E_b$ and discharge efficiency for 2D $Al_2O_3$ at the same filler loadings (of NPs and NWs) and temperature.

Barium titanate ($BaTiO_3$or BT) is an important ferroelectric ceramic and is widely used to enhance the dielectric properties of polymer matrices.[88,89] With addition of mere 1 wt.% addition of $BaTiO_3$ nanoplates, $U_d$ was increases by 100% to 9.7 J/cm$^3$. 2D fillers of similar class including 2D $NaNbO_3$ and $SrTiO_3$ have been employed for fabricating polymerdielectric composites.[90,91] Similar to $BaTiO_3$, with1 wt.% addition of $SrTiO_3$, $U_d$ was increases by 100% to 9.48 J/cm$^3$.[90] In addition to these fillers, other 2D fillers such as transition metal dichalcogenides (TMDCs)[92,93], clay minerals[94], and negatively charges metal oxide[95,96] have been successfully employed for fabrication of 2D/polymer dielectric composites.

Similar to conductive fillers, multiphase composites of insulating fillers have also been fabricated. Examples of such system are $MoS_2$/Al flakes/PVDF[97], $WS_2$/BT nanoparticles/epoxy[98], poly(vinylidene fluoride-hexafluoropropylene) (P[VDF-HFP])/montmorillonite (xMMT)/Ag[96], $Na^+$MMT/ionic liquid/PVDF[99], BT/BN/polyetherimide (PEI)[100], and BT/BN/PVDF[101]. Scope of dielectric improvement in multiphase polymer composites containing insulating fillers is more than the conducting filler base such systems. For example, BN nanosheets and BT were dispersed in N, N-dimethylformamide (DMF) and then mixed together to BT@BN particles which were then mixed with PVDF matrix. Using these hybrid fillers, $E_b$ improved to 580 kV/mm, and high energy density of 17.6 J/cm$^3$was obtained for 5 wt.% filler concentrations, which was better than binary phase composites, see Figure 14.[101] The simulated (Figure 14c-e) maximum volume current densities in the composites of BT@BN/PVDF, BN/PVDF, and BT/PVDF, are $1.12E^{-11}$, $1.16E^{-11}$, and $9.17E^{-10}$ A/cm$^2$, respectively. These current densities are directly related with breakdown process. As a result, BT@BN/PVDF composites achieved higher $E_b$ compared to binary phase composites.

## Dielectric properties of layered 2D-filler/polymer composites

Mixing 2D fillers with polymers is an easy straightforward approach to prepare the composites with dielectric properties. However, for such composites control over interface between fillers and polymers is not easy. Polymer-filler interface is probably the most important parameter to obtain the good electrical properties. Alternate route is to fabricate multilayered polymer composite structures to obtain high dielectric constant and large $E_b$. Both three layered and more than three layered composites have been fabricated for dielectric properties. Pan et al. fabricated 2D NaNbO (NN) platelets/PVDF

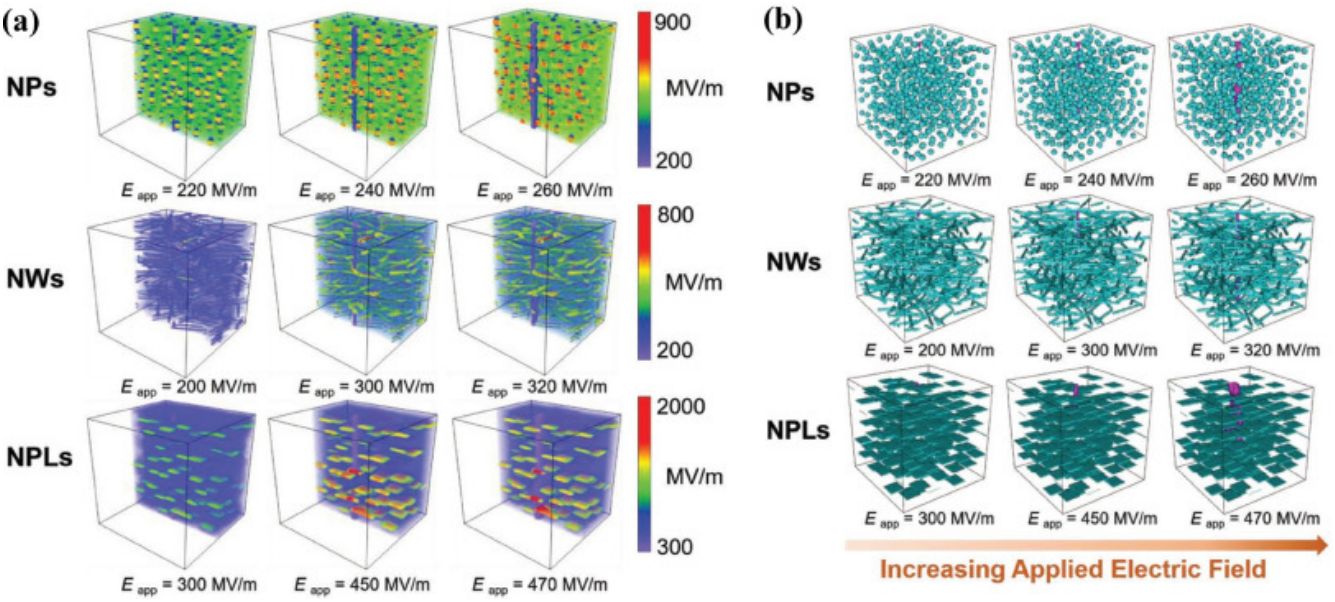


*Figure 13. (a) Electric field distribution and (b) corresponding predicted breakdown path evolution computed by phase-field simulations of the c-BCB nanocomposites with 7.5vol% $Al_2O_3$ nanoparticles, nanowires and nanoplates at 150 °C and varied applied electric fields.*[87] *Reproduced with permission from ref. 87. Copyright (2019) WILEY-VCH.*

composites for outer layers and pristine PVDF was sued as middle layer. Then all the layers were stacked according to the scheme shown in Figure 15. A high discharge energy density of 13.5 J cm at 400 MV mpower density of 2.68 MW cm, discharge energy efficiency of 66.9%, and ultrafast discharge speed of 0.127 $\mu$s was obtained. Figure 15 band c show the discharge energy density and efficiency of 3% NN/PVDF composites and 3-0-3 layered composites. 3 in 3-0-3 represents the filler volume percentage, and 0 represents the pristine PVDF. In these composites middle layer experience, the high electric filed and also prevent electrical field channels, which increase overall electric field tolerance capacity of the layered composites. Titanate filled PVDF composites as middle layer and pristine PVDF as outer layer were fabricated with 11.69 J cm and an excellent discharge efficiency of 78.95%. Composites with more than 3 layers composing of BN nanosheets and $Ba(Zr_{0.21}Ti_{0.79})O_3$ nanofibers (BZT NFs)[103] layers, rGO-P1/BN-PI[104] layers, and P(VDF-HFP)/BN[105] layers have been reported with significantly improved dielectric properties. In some cases, filler layer has also been used in multilayered structures. Zhu et al.[106] fabricated layered composites with BN as middle layer and PVDF as outer layer. Composites were fabricated through a simple layer-by-layer solution-casting process. During the casting process, BN nanosheets were aligned along the in-plane direction. Compared to the pristine PVDF, the composite films show remarkably suppressed leakage current, resulting in a high breakdown strength and a superior energy density which are 136% and 275%, respectively. Liu et al.[107] used BN nanosheets as outer layer to sandwich polycarbonate (PC) layer. The energy storage density of the composites was 5.52 J/cm$^3$ under 500 MV/m electric field at 100 °C, which is 15.10% higher than that of pure PC.

## SUMMARY AND OUTLOOK

OP2D materials has great potential for polymer dielectric composites due to their superior electrical properties and high surface area to interface with polymer matrix. For use of 2D polymer for composite applications, large scale high quality synthesis of 2D quality is a big challenge. Current synthesis methods are trade-off between large scale synthesis and structural quality of 2D materials. Liquid based synthesis methods can produce ton scale 2D materials but quality is poor due to presence of structural defects arising from violent chemical reactions. CVD can produce good quality 2D materials but scalability is a serious issue, as materials can only be grown as sheets. Currently, for polymer composites, liquid synthesis of 2D materials is preferred route, however, quality of 2D materials need to be improved in the future. For dielectric properties, conductive 2D-fillers (such as Gr, MXenes) do offer large dielectric constant values at low filler concentrations, but these composites have large dielectric loss values, low breakdown strength and low energy den-

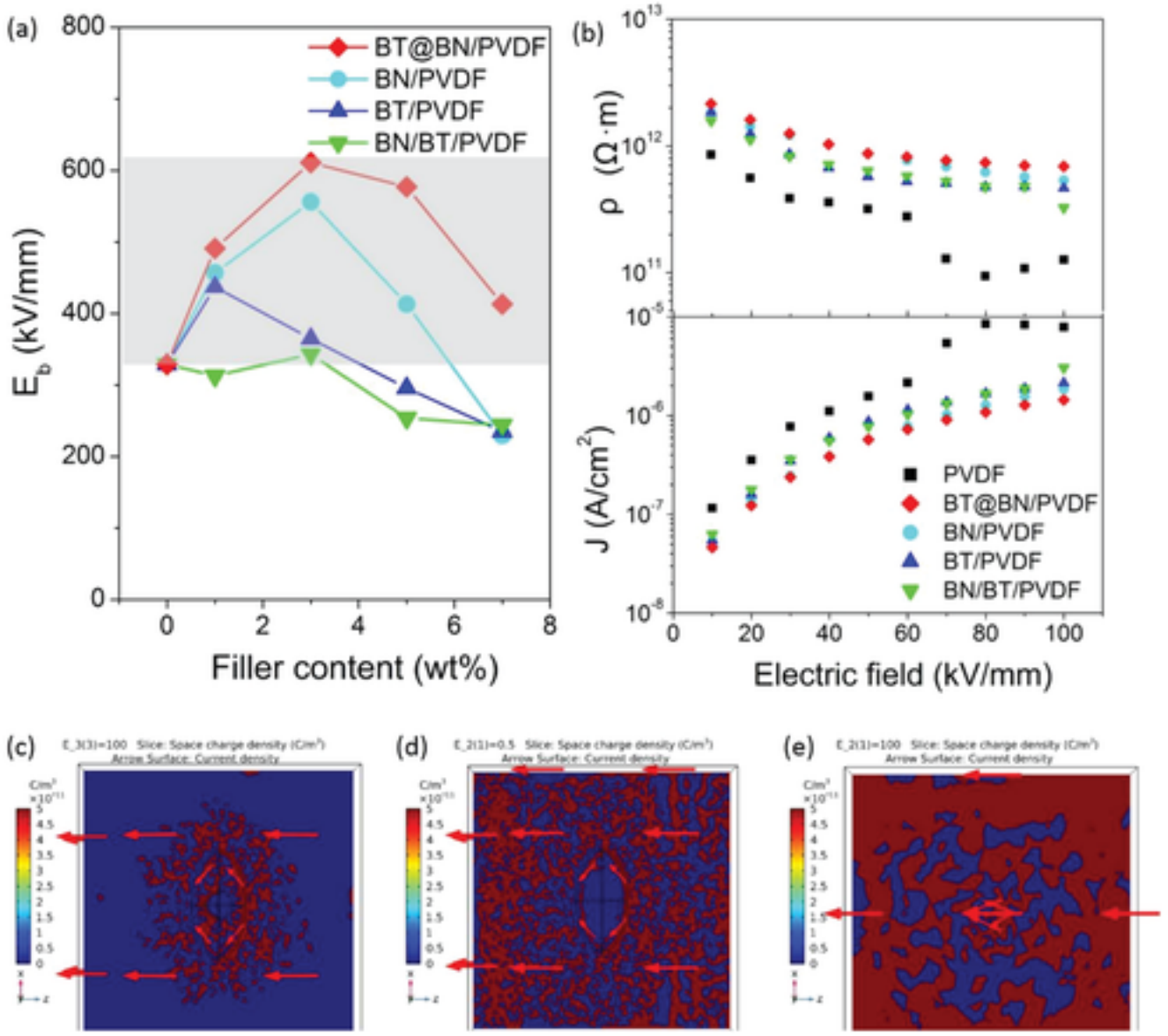


*Figure 14. (a) Variation of $E_b$ with the filler content of the four types of films. (b) Resistivity and leakage current density as a function of the electric field of the PVDF and the composite films filled with 3 wt% of fillers. (c–e) The simulated space charge density distribution in the PVDF composites filled with BT@BN, BN, and BT, respectively. The arrows indicate the direction of the electric field. The particles are in the middle position of the simulated area.*[101] *reproduced with permission from ref. 101. Copyright (2018) WILEY-VCH*

sity. Moreover, their properties are significantly influenced by frequency and external stimuli such as temperature and pressure. On the other hand, non-conductive 2D-fillers based polymer composites offer low dielectric constant value even at relatively large filler concentrations, but their dielectric loss value is very low, hence breakdown strength and energy density values are good. Moreover, dielectric properties of these composites are stable against temperature, pressure and frequency. Dielectric properties of both conductive and non-conductive 2D filler based composites can be fine-tuned by the use of multi phase and layered composites. However, to do that, a fine understanding of structure-property relationship of multi phase and layered composites need to be developed and should be the focus of future research.

## ACKNOWLEDGMENTS

The authors are thankful to the National Natural Foundation of China

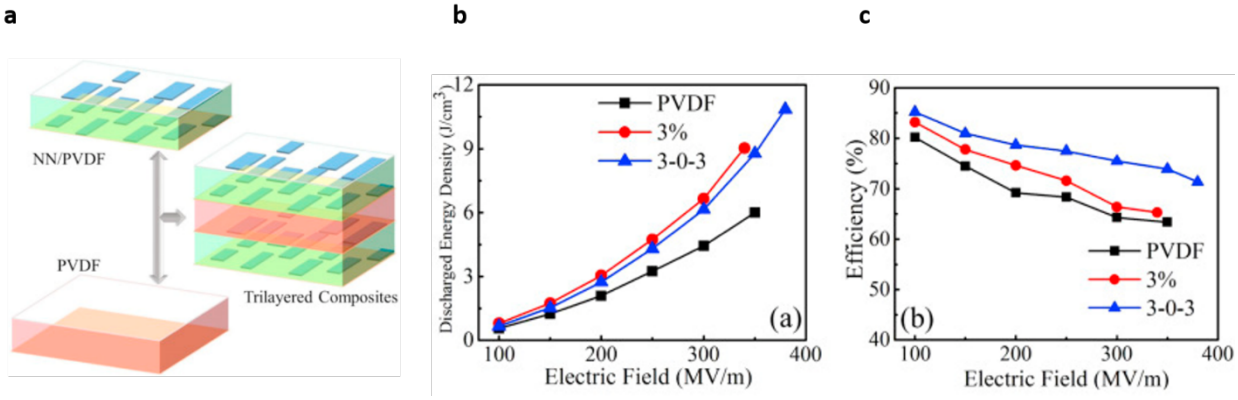


*Figure 15. Figure 15. (a) Fabrication of trilayered architecture composite films. (b) Discharged energy density, (c) efficiency of pristine PVDF, 3 vol. % NN/PVDF, and 3-0-3 composite film.*[91] *Reproduced with permission from ref. 91. Copyright (2017) Elsevier.*

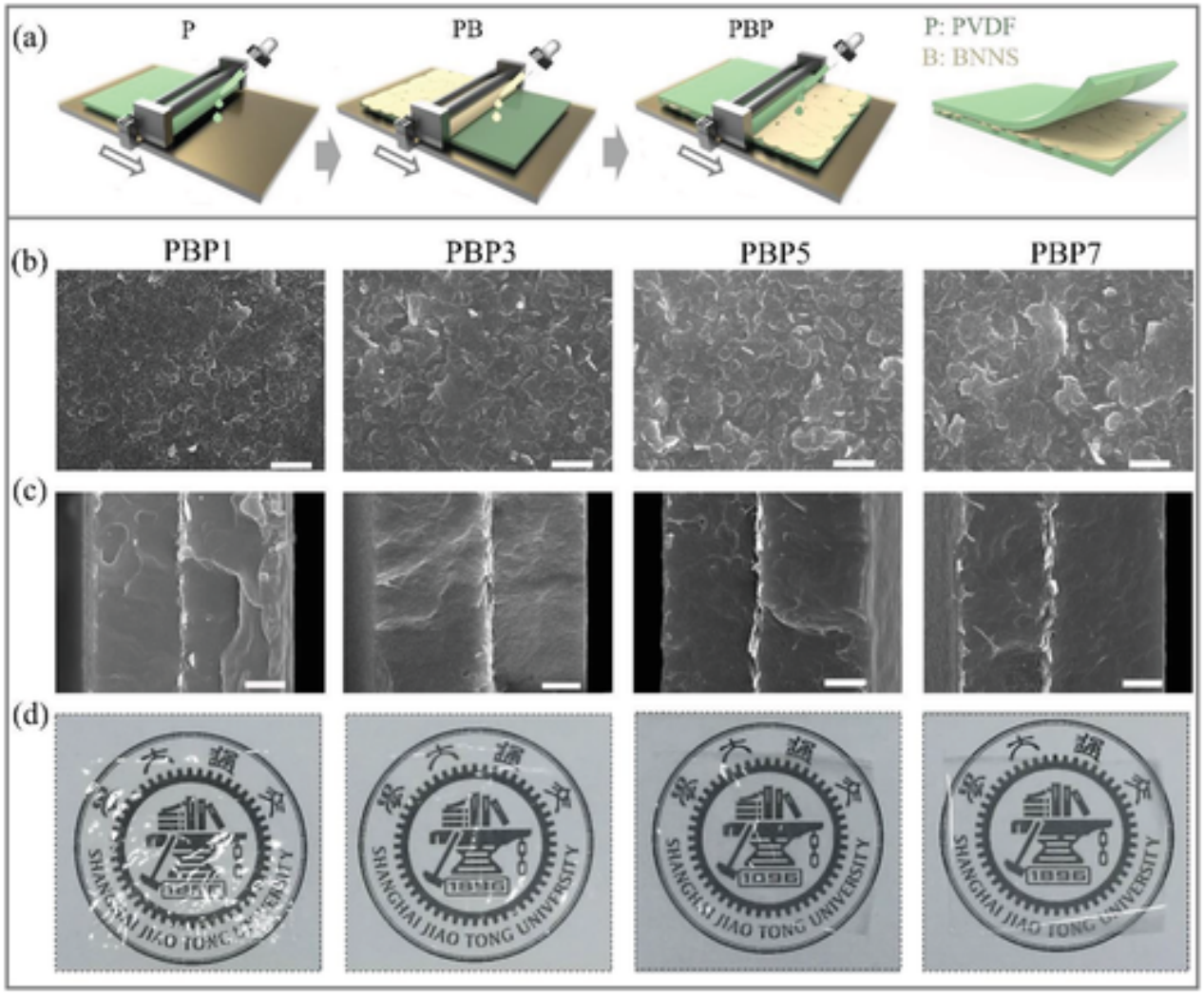


*Figure 16. Processing of PVDF/BNnanosheets/PVDF layered composites.*[106] *Reproduced with permission from ref. 106. Copyright (2019) Elsevier.*

(51803081) for their financial support. The representative authors have no conflict of interest to disclose in any capacity, either competing or financial.

## References


1) Zogb, D. Passive Electronic Components: Global Market Update. 2021; available at https://www.tti.com/content/ttiinc/en/resources/marketeye/categories/passives/me-zogbi-20210906.html.
2) Bar-Cohen, Y. Electroactive Polymers as Artificial Muscles: A Review. *Journal of Spacecraft and Rockets* **2002**, *39* (6), 822–827, DOI: 10.2514/2.3902, available at https://dx.doi.org/10.2514/2.3902.
3) Uchino, K. Piezoelectric actuators and ultrasonic motors. 1996.
4) Ni, D.; Heisser, R.; Davaji, B.; Ivy, L.; Shepherd, R.; Lal, A.
5) Laihonen, S.; Gafvert, U.; Schutte, T.; Gedde, U. DC breakdown strength of polypropylene films: area dependence and statistical behavior. *IEEE Transactions on Dielectrics and Electrical Insulation* **2007**, *14* (2), 275–286, DOI: 10.1109/tdei.2007.344604, available at https://dx.doi.org/10.1109/tdei.2007.344604.
6) Ho, J.; Ramprasad, R.; Boggs, S. Effect of Alteration of Antioxidant by UV Treatment on the Dielectric Strength of BOPP Capacitor Film. *IEEE Transactions on Dielectrics and Electrical Insulation* **2007**, *14* (5), 1295–1301, DOI: 10.1109/tdei.2007.4339492, available at https://dx.doi.org/10.1109/tdei.2007.4339492.
7) Han, Z.; Wang, Q. Recent progress on dielectric polymers and composites for capacitive energy storage. *iEnergy* **2022**, *1* (1), 50–71, DOI: 10.23919/ien.2022.0008, available at https://dx.doi.org/10.23919/ien.2022.0008.
8) Dang, Z.-M.; Shehzad, K.; Zha, J.-W.; Hussain, T.; Jun, N.; Bai, J. On Refining the Relationship between Aspect Ratio and Percolation Threshold of Practical Carbon Nanotubes/Polymer Nanocomposites. *Japanese Journal of Applied Physics* **2011**, *50* (8), 080214–080214, DOI: 10.1143/jjap.50.080214, available at https://dx.doi.org/10.1143/jjap.50.080214.
9) Shehzad, K.; Ahmad, M. N.; Hussain, T.; Mumtaz, M.; Shah, A. T.; Mujahid, A.; Wang, C.; Ellingsen, J.; Dang, Z.-M. Influence of carbon nanotube dimensions on the percolation characteristics of carbon nanotube/polymer composites. *Journal of Applied Physics* **2014**, *116* (6), 064908–064908, DOI: 10.1063/1.4892156, available at https://dx.doi.org/10.1063/1.4892156.
10) Shehzad, K.; Hakro, A. A.; Zeng, Y.; Yao, S.-H.; Xiao-Hong, Y.; Mumtaz, M.; Nadeem, K.; Khisro, N. S.; Dang, Z.-M. Two percolation thresholds and remarkably high dielectric permittivity in pristine carbon nanotube/elastomer composites. *Applied Nanoscience* **2015**, *5* (8), 969–974, DOI: 10.1007/s13204-015-0403-0, available at https://dx.doi.org/10.1007/s13204-015-0403-0.
11) Shehzad, K.; Hussain, T.; Shah, A. T.; Mujahid, A.; Ahmad, M. N.; ur Rahman Sagar, R.; Anwar, T.; Nasir, S.; Ali, A. Effect of the carbon nanotube size dispersity on the electrical properties and pressure sensing of the polymer composites. *Journal of Materials Science* **2016**, *51* (24), 11014–11020, DOI: 10.1007/s10853-016-0322-9, available at https://dx.doi.org/10.1007/s10853-016-0322-9.
12) Shehzad, K.; Xu, Y.; Gao, C.; Li, H.; Dang, Z.-M.; Hasan, T.; Luo, J.; Duan, X. Flexible Dielectric Nanocomposites with Ultrawide Zero-Temperature Coefficient Windows for Electrical Energy Storage and Conversion under Extreme Conditions. *ACS Applied Materials & Interfaces* **2017**, *9* (8), 7591–7600, DOI: 10.1021/acsami.6b14984, available at https://dx.doi.org/10.1021/acsami.6b14984.
13) Shehzad, K.; Zha, J.-W.; Zhang, Z.-F.; Yuan, J.-K.; Dang, Z.-M. Piezoresistive Behavior of Electrically Conductive Carbon Fillers/Thermoplastic Elastomer Nanocomposites. *Journal of Advanced Physics* **2013**, *2* (1), 70–74, DOI: 10.1166/jap.2013.1038, available at https://dx.doi.org/10.1166/jap.2013.1038.
14) Zha, J.-W.; Shehzad, K.; Li, W.-K.; Dang, Z.-M. The effect of aspect ratio on the piezoresistive behavior of the multiwalled carbon nanotubes/thermoplastic elastomer nanocomposites. *Journal of Applied Physics* **2013**, *113* (1), 014102–014102, DOI: 10.1063/1.4772747, available at https://dx.doi.org/10.1063/1.4772747.
15) Hussain, T.; Jabeen, S.; Shehzad, K.; Mujahid, A.; Ahmad, M. N.; Farooqi, Z. H.; Raza, M. H. Polyaniline/silver decorated-MWCNT composites with enhanced electrical and thermal properties. *Polymer Composites* **2018**, *39* (S3), E1346–E1353.
16) Shehzad, K.; Ul-Haq, A.; Ahmad, S.; Mumtaz, M.; Hussain, T.; Mujahid, A.; Shah, A. T.; Choudhry, M. Y.; Khokhar, I.; Ul-Hassan, S.; Nawaz, F.; ur Rahman, F.; Butt, Y.; Pervaiz, M. All-organic PANI–DBSA/PVDF dielectric composites with unique electrical properties. *Journal of Materials Science* **2013**, *48* (10), 3737–3744, DOI: 10.1007/s10853-013-7172-5, available at https://dx.doi.org/10.1007/s10853-013-7172-5.
17) Silakaew, K.; Swatsitang, E.; Thongbai, P. Novel polymer composites of RuO2@nBaTiO3/PVDF with a high dielectric constant. *Ceramics International* **2022**, DOI: 10.1016/j.ceramint.2022.03.173, available at https://dx.doi.org/10.1016/j.ceramint.2022.03.173.
18) Abdelhamied, M. M.; Abdelreheem, A. M.; Atta, A. Influence of ion beam and silver nanoparticles on dielectric properties of flexible PVA/PANI polymer composite films. *Plastics, Rubber and Composites* **2022**, *51* (1), 1–12, DOI: 10.1080/14658011.2021.1928998, available at https://dx.doi.org/10.1080/14658011.2021.1928998.
19) Guo, Y.; Wu, S.; Liu, S.; Xu, J.; Pawlikowska, E.; Szafran, M.; Rydosz, A.; Gao, F. Enhanced dielectric tunability and energy storage density of sandwich-structured Ba0.6Sr0.4TiO3/PVDF composites. *Materials Letters* **2022**, *306*, 130910–130910, DOI: 10.1016/j.matlet.2021.130910, available at https://dx.doi.org/10.1016/j.matlet.2021.130910.
20) Shanmugasundram, H. P. P. V.; Jayamani, E.; Soon, K. H. A comprehensive review on dielectric composites: Classification of dielectric composites. 2022; available at https://dx.doi.org/10.1016/j.rser.2022.112075.
21) Ali, A.; Shehzad, K.; Guo, H.; Wang, Z.; Wang, P.; Qadir, A.; Hu, W.; Ren, T.; Yu, B.; Xu, Y. High-performance, flexible graphene/ultra-thin silicon ultra-violet image sensor. *2017 IEEE International Electron Devices Meeting (IEDM)* **2017**,
22) Guo, H.; Li, L.; Liu, W.; Sun, Y.; Xu, L.; Ali, A.; Liu, Y.; Wu, C.; Shehzad, K.; Yin, W.-Y.; Xu, Y. All-Two-Dimensional-Material Hot Electron Transistor. *IEEE Electron Device Letters* **2018**, *39* (4), 634–637, DOI: 10.1109/led.2018.2810272, available at https://dx.doi.org/10.1109/led.2018.2810272.
23) Liu, W.; Guo, H.; Li, W.; Wan, X.; Bodepudi, S. C.; Shehzad, K.; Xu, Y. Light-induced negative differential resistance in gate-controlled graphene-silicon photodiode. *Applied Physics Letters* **2018**, *112* (20), 201109–201109, DOI: 10.1063/1.5026382, available at https://dx.doi.org/10.1063/1.5026382.
24) Pham, P. V.; Bodepudi, S. C.; Shehzad, K.; Liu, Y.; Xu, Y.; Yu, B.; Duan, X. 2D Heterostructures for Ubiquitous Electronics and Optoelectronics: Principles, Opportunities, and Challenges. *Chemical Reviews* **2022**, *122* (6), 6514–6613, DOI: 10.1021/acs.chemrev.1c00735, available at https://dx.doi.org/10.1021/acs.chemrev.1c00735.
25) Sagar, R. U. R.; Shehzad, K.; Ali, A.; Stadler, F. J.; Khan, Q.; Zhao, J.; Wang, X.; Zhang, M. Defect-induced, temperature-independent, tunable magnetoresistance of partially fluorinated graphene foam. *Carbon* **2019**, *143*, 179–188, DOI: 10.1016/j.carbon.2018.11.003, available at https://dx.doi.org/10.1016/j.carbon.

2018.11.003.
26) Shehzad, K. et al. Designing an Efficient Multimode Environmental Sensor Based on Graphene-Silicon Heterojunction. *Advanced Materials Technologies* **2017**, *2* (4), 1600262–1600262, DOI: 10.1002/admt.201600262, available at https://dx.doi.org/10.1002/admt.201600262.
27) Shehzad, K.; Xu, Y. Graphene light-field camera. *Nature Photonics* **2020**, *14* (3), 134–136, DOI: 10.1038/s41566-020-0597-x, available at https://dx.doi.org/10.1038/s41566-020-0597-x.
28) Xu, Y.; Ali, A.; Shehzad, K.; Meng, N.; Xu, M.; Zhang, Y.; Wang, X.; Jin, C.; Wang, H.; Guo, Y.; Yang, Z.; Yu, B.; Liu, Y.; He, Q.; Duan, X.; Wang, X.; Tan, P.-H.; Hu, W.; Lu, H.; Hasan, T. Solvent-Based Soft-Patterning of Graphene Lateral Heterostructures for Broadband High-Speed Metal–Semiconductor–Metal Photodetectors. *Advanced Materials Technologies* **2017**, *2* (2), 1600241–1600241, DOI: 10.1002/admt.201600241, available at https://dx.doi.org/10.1002/admt.201600241.
29) Glavin, N. R.; Rao, R.; Varshney, V.; Bianco, E.; Apte, A.; Roy, A.; Ringe, E.; Ajayan, P. M. Emerging Applications of Elemental 2D Materials. *Advanced Materials* **2020**, *32* (7), 1904302–1904302, DOI: 10.1002/adma.201904302, available at https://dx.doi.org/10.1002/adma.201904302.
30) Zhang, X.; Hou, L.; Ciesielski, A.; Samorì, P. 2D Materials Beyond Graphene for High-Performance Energy Storage Applications. *Advanced Energy Materials* **2016**, *6* (23), 1600671–1600671, DOI: 10.1002/aenm.201600671, available at https://dx.doi.org/10.1002/aenm.201600671.
31) Chang, C. et al. Recent Progress on Two-Dimensional Materials. *Acta Physico Chimica Sinica* **2021**, *0* (0), 2108017–0, DOI: 10.3866/pku.whxb202108017, available at https://dx.doi.org/10.3866/pku.whxb202108017.
32) Li, J.; Liu, X.; Feng, Y.; Yin, J. Recent progress in polymer/two-dimensional nanosheets composites with novel performances. *Progress in Polymer Science* **2022**, *126*, 101505–101505, DOI: 10.1016/j.progpolymsci.2022.101505, available at https://dx.doi.org/10.1016/j.progpolymsci.2022.101505.
33) Sanes, J.; Sánchez, C.; Pamies, R.; Avilés, M.-D.; Bermúdez, M.-D. Extrusion of Polymer Nanocomposites with Graphene and Graphene Derivative Nanofillers: An Overview of Recent Developments. *Materials* **2020**, *13* (3), 549–549, DOI: 10.3390/ma13030549, available at https://dx.doi.org/10.3390/ma13030549.
34) Hu, J.; Zhang, S.; Tang, B. 2D filler-reinforced polymer nanocomposite dielectrics for high-k dielectric and energy storage applications. *Energy Storage Materials* **2021**, *34*, 260–281, DOI: 10.1016/j.ensm.2020.10.001, available at https://dx.doi.org/10.1016/j.ensm.2020.10.001.
35) Shen, X.; Zheng, Q.; Kim, J.-K. Rational design of two-dimensional nanofillers for polymer nanocomposites toward multifunctional applications. *Progress in Materials Science* **2021**, *115*, 100708–100708, DOI: 10.1016/j.pmatsci.2020.100708, available at https://dx.doi.org/10.1016/j.pmatsci.2020.100708.
36) Uyor, U. O.; Popoola, A. P.; Popoola, O.; Aigbodion, V. S. Energy storage and loss capacity of graphene-reinforced poly(vinylidene fluoride) nanocomposites from electrical and dielectric properties perspective: A review. *Advances in Polymer Technology* **2018**, *37* (8), 2838–2858, DOI: 10.1002/adv.21956, available at https://dx.doi.org/10.1002/adv.21956.
37) Avishan, N.; Hussain, N.; Nosheen, F. Large-scale Graphene Production and Transfer for Industrial Applications. *Materials Innovations 2022* (1), 15–25, DOI: 10.54738/MI.2022.2102, available at http://doi.org/10.54738/MI.2022.2102.
38) Hernandez, Y.; Nicolosi, V.; Lotya, M.; Blighe, F. M.; Sun, Z.; De, S.; McGovern, I. T.; Holland, B.; Byrne, M.; Gun'Ko, Y. K.; Boland, J. J.; Niraj, P.; Duesberg, G.; Krishnamurthy, S.; Goodhue, R.; Hutchison, J.; Scardaci, V.; Ferrari, A. C.; Coleman, J. N. High-yield production of graphene by liquid-phase exfoliation of graphite. *Nature Nanotechnology* **2008**, *3* (9), 563–568, DOI: 10.1038/nnano.2008.215, available at https://dx.doi.org/10.1038/nnano.2008.215.
39) Zhou, K.-G.; Mao, N.-N.; Wang, H.-X.; Peng, Y.; Zhang, H.-L. A Mixed-Solvent Strategy for Efficient Exfoliation of Inorganic Graphene Analogues. *Angewandte Chemie* **2011**, *123* (46), 11031–11034, DOI: 10.1002/ange.201105364, available at https://dx.doi.org/10.1002/ange.201105364.
40) Lotya, M.; Hernandez, Y.; King, P. J.; Smith, R. J.; Nicolosi, V.; Karlsson, L. S.; Blighe, F. M.; De, S.; Wang, Z.; McGovern, I. T.; Duesberg, G. S.; Coleman, J. N. Liquid Phase Production of Graphene by Exfoliation of Graphite in Surfactant/Water Solutions. *Journal of the American Chemical Society* **2009**, *131* (10), 3611–3620, DOI: 10.1021/ja807449u, available at https://dx.doi.org/10.1021/ja807449u.
41) Coleman, J. N.; et al. et al., ChemInform Abstract: Two-Dimensional Nanosheets Produced by Liquid Exfoliation of Layered Materials. *ChemInform* **2011**, *42* (18), no–no, DOI: 10.1002/chin.201118179, available at https://dx.doi.org/10.1002/chin.201118179.
42) Hanlon, D. et al. Liquid exfoliation of solvent-stabilized few-layer black phosphorus for applications beyond electronics. *Nature Communications* **2015**, *6* (1), 8563–8563, DOI: 10.1038/ncomms9563, available at https://dx.doi.org/10.1038/ncomms9563.
43) Paton, K. R. et al. Scalable production of large quantities of defect-free few-layer graphene by shear exfoliation in liquids. *Nature Materials* **2014**, *13* (6), 624–630, DOI: 10.1038/nmat3944, available at https://dx.doi.org/10.1038/nmat3944.
44) Hummers, W. S.; Offeman, R. E. Preparation of Graphitic Oxide. *Journal of the American Chemical Society* **1958**, *80* (6), 1339–1339, DOI: 10.1021/ja01539a017, available at https://dx.doi.org/10.1021/ja01539a017.
45) Li, X.; Hao, X.; Zhao, M.; Wu, Y.; Yang, J.; Tian, Y.; Qian, G. Exfoliation of Hexagonal Boron Nitride by Molten Hydroxides. *Advanced Materials* **2013**, *25* (15), 2200–2204, DOI: 10.1002/adma.201204031, available at https://dx.doi.org/10.1002/adma.201204031.
46) Jing, L.; Li, H.; Tay, R. Y.; Sun, B.; Tsang, S. H.; Cometto, O.; Lin, J.; Teo, E. H. T.; Tok, A. I. Y. Biocompatible Hydroxylated Boron Nitride Nanosheets/Poly(vinyl alcohol) Interpenetrating Hydrogels with Enhanced Mechanical and Thermal Responses. *ACS Nano* **2017**, *11* (4), 3742–3751, DOI: 10.1021/acsnano.6b08408, available at https://dx.doi.org/10.1021/acsnano.6b08408.
47) Schöllhorn, R. ChemInform Abstract: REVERSIBLE TOPOTACTIC REDOX REACTIONS OF SOLIDS THROUGH ELECTRON/ION TRANSFER. *Chemischer Informationsdienst* **1981**, *12* (11), 983–1003.
48) Zhu, G.; Liu, J.; Zheng, Q.; Zhang, R.; Li, D.; Banerjee, D.; Cahill, D. G. Tuning thermal conductivity in molybdenum disulfide by electrochemical intercalation. *Nature Communications* **2016**, *7* (1), 1–9, DOI: 10.1038/ncomms13211, available at https://dx.doi.org/10.1038/ncomms13211.
49) Zeng, Z.; Sun, T.; Zhu, J.; Huang, X.; Yin, Z.; Lu, G.; Fan, Z.; Yan, Q.; Hng, H. H.; Zhang, H. An Effective Method for the Fabrication of Few-Layer-Thick Inorganic Nanosheets. *Angewandte Chemie* **2012**, *124* (36), 9186–9190, DOI: 10.1002/ange.201204208, available at https://dx.doi.org/10.1002/ange.201204208.
50) Peng, J.; Wu, J.; Li, X.; Zhou, Y.; Yu, Z.; Guo, Y.; Wu, J.; Lin, Y.; Li, Z.; Wu, X.; Wu, C.; Xie, Y. Very Large-Sized Transition Metal Dichalcogenides Monolayers from Fast Exfoliation by Manual Shaking. *Journal of the American Chemical Society* **2017**, *139* (26), 9019–9025, DOI: 10.1021/jacs.7b04332, available at https://dx.doi.org/10.1021/jacs.7b04332.

51) Tsai, H. L.; Heising, J.; Schindler, J. L.; Kannewurf, C. R.; Kanatzidis, M. G. Exfoliated—restacked phase of WS2. *Chemistry of materials* **1997**, *9* (4), 879–882.
52) Gordon, R.; Yang, D.; Crozier, E.; Jiang, D.; Frindt, R. Structures of exfoliated single layers of WS 2, MoS 2, and MoSe 2 in aqueous suspension. *Physical Review B* **2002**, (12), 125407–125407.
53) Zhou, J. et al. A library of atomically thin metal chalcogenides. *Nature* **2018**, *556* (7701), 355–359, DOI: 10.1038/s41586-018-0008-3, available at https://dx.doi.org/10.1038/s41586-018-0008-3.
54) Tang, L.; Tan, J.; Nong, H.; Liu, B.; Cheng, H. M. *Chemical Vapor Deposition Growth of Two-Dimensional Compound Materials: Controllability, Material Quality, and Growth Mechanism. Accounts of Materials Research 2021* (1), 36–47.
55) Dang, Z.-M.; Yuan, J.-K.; Zha, J.-W.; Zhou, T.; Li, S.-T.; Hu, G.-H. Fundamentals, processes and applications of high-permittivity polymer–matrix composites. *Progress in Materials Science* **2012**, *57* (4), 660–723, DOI: 10.1016/j.pmatsci.2011.08.001, available at https://dx.doi.org/10.1016/j.pmatsci.2011.08.001.
56) Zhang, X.; Zhang, J.; Xia, L.; Li, C.; Wang, J.; Xu, F.; Zhang, X.; Wu, H.; Guo, S. Simple and Consecutive Melt Extrusion Method to Fabricate Thermally Conductive Composites with Highly Oriented Boron Nitrides. *ACS Applied Materials & Interfaces* **2017**, *9* (27), 22977–22984, DOI: 10.1021/acsami.7b05866, available at https://dx.doi.org/10.1021/acsami.7b05866.
57) Nan, C. W. Physics of inhomogeneous inorganic materials. Progress in materials science. *Progress in materials science* **1993**, *37*, 1–116, DOI: 10.1016/0079-6425(93)90004-5, available at https://doi.org/10.1016/0079-6425(93)90004-5.
58) Zakri, T.; Laurent, J.-P.; Vauclin, M. Theoretical evidence for 'Lichtenecker's mixture formulae' based on the effective medium theory. *Journal of Physics D: Applied Physics* **1998**, *31* (13), 1589–1594, DOI: 10.1088/0022-3727/31/13/013, available at https://dx.doi.org/10.1088/0022-3727/31/13/013.
59) Jayasundere, N.; Smith, B. V. Dielectric constant for binary piezoelectric 0-3 composites. *Journal of Applied Physics* **1993**, *73* (5), 2462–2466, DOI: 10.1063/1.354057, available at https://dx.doi.org/10.1063/1.354057.
60) Li, Y. C.; Tjong, S. C.; Li, R. K. Y. Electrical conductivity and dielectric response of poly(vinylidene fluoride)–graphite nanoplatelet composites. *Synthetic Metals* **2010**, *160* (17-18), 1912–1919, DOI: 10.1016/j.synthmet.2010.07.009, available at https://dx.doi.org/10.1016/j.synthmet.2010.07.009.
61) Chu, L.; Xue, Q.; Sun, J.; Xia, F.; Xing, W.; Xia, D.; Dong, M. Porous graphene sandwich/poly(vinylidene fluoride) composites with high dielectric properties. *Composites Science and Technology* **2013**, *86*, 70–75, DOI: 10.1016/j.compscitech.2013.07.001, available at https://dx.doi.org/10.1016/j.compscitech.2013.07.001.
62) Xu, P.; Gui, H.; Wang, X.; Hu, Y.; Ding, Y. Improved dielectric properties of nanocomposites based on polyvinylidene fluoride and ionic liquid-functionalized graphene. *Composites Science and Technology* **2015**, *117*, 282–288, DOI: 10.1016/j.compscitech.2015.06.023, available at https://dx.doi.org/10.1016/j.compscitech.2015.06.023.
63) Weng, L.; Wang, T.; Liu, L. A study on the structure and properties of poly(vinylidene fluoride)/graphite microsheet composite films. *Journal of Composite Materials* **2017**, *51* (27), 3769–3778, DOI: 10.1177/0021998317693675, available at https://dx.doi.org/10.1177/0021998317693675.
64) Yang, D.; Kong, X.; Ni, Y.; Ruan, M.; Huang, S.; Shao, P.; Guo, W.; Zhang, L. Improved Mechanical and Electrochemical Properties of XNBR Dielectric Elastomer Actuator by Poly(dopamine) Functionalized Graphene Nano-Sheets. *Polymers* **2019**, *11* (2), 218–218, DOI: 10.3390/polym11020218, available at https://dx.doi.org/10.3390/polym11020218.
65) Lv, Q.-C.; Li, Y.; Zhong, Z.-K.; Wu, H.-J.; He, F.-A.; Lam, K.-H. Preparation and dielectric properties of novel composites based on oxidized styrene-butadienestyrene copolymer and polyaniline modified exfoliated graphite nanoplates. *Applied Surface Science* **2018**, *441*, 945–954, DOI: 10.1016/j.apsusc.2018.02.034, available at https://dx.doi.org/10.1016/j.apsusc.2018.02.034.
66) He, F.; Lau, S.; Chan, H. L.; Fan, J. High Dielectric Permittivity and Low Percolation Threshold in Nanocomposites Based on Poly(vinylidene fluoride) and Exfoliated Graphite Nanoplates. *Advanced Materials* **2009**, *21* (6), 710–715, DOI: 10.1002/adma.200801758, available at https://dx.doi.org/10.1002/adma.200801758.
67) Li, H.; Chen, Z.; Liu, L.; Chen, J.; Jiang, M.; Xiong, C. Poly(vinyl pyrrolidone)-coated graphene/poly(vinylidene fluoride) composite films with high dielectric permittivity and low loss. *Composites Science and Technology* **2015**, *121*, 49–55, DOI: 10.1016/j.compscitech.2015.11.001, available at https://dx.doi.org/10.1016/j.compscitech.2015.11.001.
68) Wang, D.; Bao, Y.; Zha, J.-W.; Zhao, J.; Dang, Z.-M.; Hu, G.-H. Improved Dielectric Properties of Nanocomposites Based on Poly(vinylidene fluoride) and Poly(vinyl alcohol)-Functionalized Graphene. *ACS Applied Materials & Interfaces* **2012**, *4* (11), 6273–6279, DOI: 10.1021/am3018652, available at https://dx.doi.org/10.1021/am3018652.
69) Wang, J.; Wu, J.; Xu, W.; Zhang, Q.; Fu, Q. Preparation of poly(vinylidene fluoride) films with excellent electric property, improved dielectric property and dominant polar crystalline forms by adding a quaternary phosphorus salt functionalized graphene. *Composites Science and Technology* **2014**, *91*, 1–7, DOI: 10.1016/j.compscitech.2013.11.002, available at https://dx.doi.org/10.1016/j.compscitech.2013.11.002.
70) Fang, X.; Liu, X.; Cui, Z.-K.; Qian, J.; Pan, J.; Li, X.; Zhuang, Q. Preparation and properties of thermostable well-functionalized graphene oxide/polyimide composite films with high dielectric constant, low dielectric loss and high strength via in situ polymerization. *Journal of Materials Chemistry A* **2015**, *3* (18), 10005–10012, DOI: 10.1039/c5ta00943j, available at https://dx.doi.org/10.1039/c5ta00943j.
71) Yuan, J.; Luna, A.; Neri, W.; Zakri, C.; Schilling, T.; Colin, A.; Poulin, P. Graphene liquid crystal retarded percolation for new high-k materials. *Nature Communications* **2015**, *6* (1), 8700–8700, DOI: 10.1038/ncomms9700, available at https://dx.doi.org/10.1038/ncomms9700.
72) Liu, H.; Xu, P.; Yao, H.; Chen, W.; Zhao, J.; Kang, C.; Bian, Z.; Gao, L.; Guo, H. Controllable reduction of graphene oxide and its application during the fabrication of high dielectric constant composites. *Applied Surface Science* **2017**, *420*, 390–398, DOI: 10.1016/j.apsusc.2017.05.181, available at https://dx.doi.org/10.1016/j.apsusc.2017.05.181.
73) Li, W.; Song, Z.; Qian, J.; Tan, Z.; Chu, H.; Wu, X.; Nie, W.; Ran, X. Enhancing conjugation degree and interfacial interactions to enhance dielectric properties of noncovalent functionalized graphene/poly (vinylidene fluoride) composites. *Carbon* **2019**, *141*, 728–738, DOI: 10.1016/j.carbon.2018.10.030, available at https://dx.doi.org/10.1016/j.carbon.2018.10.030.
74) Tu, S.; Jiang, Q.; Zhang, X.; Alshareef, H. N. Large Dielectric Constant Enhancement in MXene Percolative Polymer Composites. *ACS Nano* **2018**, *12* (4), 3369–3377, DOI: 10.1021/acsnano.7b08895, available at https://dx.doi.org/10.1021/acsnano.7b08895.
75) He, F.; Lau, S.; Chan, H. L.; Fan, J. High Dielectric Permittivity and Low Percolation Threshold in Nanocomposites Based on Poly(vinylidene fluoride) and Exfoliated Graphite Nanoplates. *Advanced Materials* **2009**, *21* (6), 710–715, DOI: 10.1002/adma.200801758, available

at https://dx.doi.org/10.1002/adma.200801758.
76) Ke, K.; McMaster, M.; Christopherson, W.; Singer, K. D.; Manas-Zloczower, I. Effects of branched carbon nanotubes and graphene nanoplatelets on dielectric properties of thermoplastic polyurethane at different temperatures. *Composites Part B: Engineering* **2019**, *166*, 673–680, DOI: 10.1016/j.compositesb.2019.03.005, available at https://dx.doi.org/10.1016/j.compositesb.2019.03.005.
77) Zhu, P.; Weng, L.; Zhang, X.; Wang, X.; Guan, L.; Liu, L. Graphene@poly(dopamine)-Ag core–shell nanoplatelets as fillers to enhance the dielectric performance of polymer composites. *Journal of Materials Science* **2020**, *55* (18), 7665–7679, DOI: 10.1007/s10853-020-04557-y, available at https://dx.doi.org/10.1007/s10853-020-04557-y.
78) Feng, Y.; Deng, Q.; Peng, C.; Wu, Q. High dielectric and breakdown properties achieved in ternary BaTiO3/MXene/PVDF nanocomposites with low-concentration fillers from enhanced interface polarization. *Ceramics International* **2019**, *45* (6), 7923–7930, DOI: 10.1016/j.ceramint.2019.01.104, available at https://dx.doi.org/10.1016/j.ceramint.2019.01.104.
79) Deng, Q.; Feng, Y.; Li, W.; Xu, X.; Peng, C.; Wu, Q. Strong interface effect induced high-k property in polymer based ternary composites filled with 2D layered Ti3C2 MXene nanosheets. *Journal of Materials Science: Materials in Electronics* **2019**, *30* (10), 9106–9113, DOI: 10.1007/s10854-019-01239-7, available at https://dx.doi.org/10.1007/s10854-019-01239-7.
80) Wang, J.; Chen, H.; Li, X.; Zhang, C.; Yu, W.; Zhou, L.; Yang, Q.; Shi, Z.; Xiong, C. Flexible dielectric film with high energy density based on chitin/boron nitride nanosheets. *Chemical Engineering Journal* **2020**, *383*, 123147–123147, DOI: 10.1016/j.cej.2019.123147, available at https://dx.doi.org/10.1016/j.cej.2019.123147.
81) Zhang, X.; Chen, H.; Ye, H.; Liu, A.; Xu, L. Enhanced interfacial polarization in poly(vinylidene fluoride-chlorotrifluoroethylene) nanocomposite with parallel boron nitride nanosheets. *Nanotechnology* **2020**, *31* (16), 165703–165703, DOI: 10.1088/1361-6528/ab69b4, available at https://dx.doi.org/10.1088/1361-6528/ab69b4.
82) Liu, F.; Li, Q.; Li, Z.; Liu, Y.; Dong, L.; Xiong, C.; Wang, Q. Poly(methyl methacrylate)/boron nitride nanocomposites with enhanced energy density as high temperature dielectrics. *Composites Science and Technology* **2017**, *142*, 139–144, DOI: 10.1016/j.compscitech.2017.02.006, available at https://dx.doi.org/10.1016/j.compscitech.2017.02.006.
83) Li, Q.; Chen, L.; Gadinski, M. R.; Zhang, S.; Zhang, G.; Li, H. U.; Iagodkine, E.; Haque, A.; Chen, L.-Q.; Jackson, T. N.; Wang, Q. Flexible high-temperature dielectric materials from polymer nanocomposites. *Nature* **2015**, *523* (7562), 576–579, DOI: 10.1038/nature14647, available at https://dx.doi.org/10.1038/nature14647.
84) Wang, J.; Xie, Y.; Liu, J.; Zhang, Z.; Zhang, Y. Towards high efficient nanodielectrics from linear ferroelectric P(VDF-TrFE-CTFE)-g-PMMA matrix and exfoliated mica nanosheets. *Applied Surface Science* **2019**, *469*, 437–445, DOI: 10.1016/j.apsusc.2018.11.073, available at https://dx.doi.org/10.1016/j.apsusc.2018.11.073.
85) Ji, W.; Deng, H.; Sun, C.; Fu, Q. Nickel hydroxide as novel filler for high energy density dielectric polymer composites. *Composites Science and Technology* **2019**, *172*, 117–124, DOI: 10.1016/j.compscitech.2019.01.010, available at https://dx.doi.org/10.1016/j.compscitech.2019.01.010.
86) Shen, Y.; Du, J.; Zhang, X.; Huang, X.; Song, Y.; Wu, H.; Lin, Y.; Li, M.; Nan, C.-W. Enhanced breakdown strength and suppressed leakage current of polyvinylidene fluoride nanocomposites by two-dimensional ZrO<SUB>2</SUB> nanosheets. *Materials Express* **2016**, *6* (3), 277–282, DOI: 10.1166/mex.2016.1309, available at https://dx.doi.org/10.1166/mex.2016.1309.
87) Li, H.; Ai, D.; Ren, L.; Yao, B.; Han, Z.; Shen, Z.; Wang, J.; Chen, L.-Q.; Wang, Q. Scalable Polymer Nanocomposites with Record High-Temperature Capacitive Performance Enabled by Rationally Designed Nanostructured Inorganic Fillers. *Advanced Materials* **2019**, *31* (23), 1900875–1900875, DOI: 10.1002/adma.201900875, available at https://dx.doi.org/10.1002/adma.201900875.
88) Bouharras, F. E.; Raihane, M.; Ameduri, B. Recent progress on core-shell structured BaTiO3@polymer/fluorinated polymers nanocomposites for high energy storage: Synthesis, dielectric properties and applications. *Progress in Materials Science* **2020**, *113*, 100670–100670, DOI: 10.1016/j.pmatsci.2020.100670, available at https://dx.doi.org/10.1016/j.pmatsci.2020.100670.
89) Gao, F.; Zhang, K.; Guo, Y.; Xu, J.; Szafran, M. (Ba, Sr)TiO3/polymer dielectric composites–progress and perspective. *Progress in Materials Science* **2021**, *121*, 100813–100813, DOI: 10.1016/j.pmatsci.2021.100813, available at https://dx.doi.org/10.1016/j.pmatsci.2021.100813.
90) Zhang, R.; Sheng, Q.; Ye, L.; Long, S.; Zhou, B.; Wen, F.; Yang, J.; Wang, G.; Bai, W. Two-dimensional SrTiO3 platelets induced the improvement of energy storage performance in polymer composite films at low electric fields. *Ceramics International* **2022**, *48* (5), 7145–7152, DOI: 10.1016/j.ceramint.2021.11.274, available at https://dx.doi.org/10.1016/j.ceramint.2021.11.274.
91) Pan, Z.; Liu, B.; Zhai, J.; Yao, L.; Yang, K.; Shen, B. NaNbO3 two-dimensional platelets induced highly energy storage density in trilayered architecture composites. *Nano Energy* **2017**, *40*, 587–595, DOI: 10.1016/j.nanoen.2017.09.004, available at https://dx.doi.org/10.1016/j.nanoen.2017.09.004.
92) Chen, H.; Li, X.; Yu, W.; Wang, J.; Shi, Z.; Xiong, C.; Yang, Q. Chitin/MoS<sub>2</sub> Nanosheet Dielectric Composite Films with Significantly Enhanced Discharge Energy Density and Efficiency. *Biomacromolecules* **2020**, *21* (7), 2929–2937, DOI: 10.1021/acs.biomac.0c00732, available at https://dx.doi.org/10.1021/acs.biomac.0c00732.
93) Cheng, D.; Wang, H.; Liu, B.; Wang, S.; Li, Y.; Xia, Y.; Xiong, C. Dielectric properties and energy-storage performance of two-dimensional molybdenum disulfide nanosheets/polyimide composite films. *Journal of Applied Polymer Science* **2019**, *136* (39), 47991–47991, DOI: 10.1002/app.47991, available at https://dx.doi.org/10.1002/app.47991.
94) Fu, Y.; Wang, Y.; Wang, S.; Gao, Z.; Xiong, C. Enhanced breakdown strength and energy storage of PVDF-based dielectric composites by incorporating exfoliated mica nanosheets. *Polymer Composites* **2019**, *40* (5), 2088–2094, DOI: 10.1002/pc.24991, available at https://dx.doi.org/10.1002/pc.24991.
95) Wen, R.; Guo, J.; Zhao, C.; Liu, Y. Nanocomposite Capacitors with Significantly Enhanced Energy Density and Breakdown Strength Utilizing a Small Loading of Monolayer Titania. *Advanced Materials Interfaces* **2018**, *5* (3), 1701088–1701088, DOI: 10.1002/admi.201701088, available at https://dx.doi.org/10.1002/admi.201701088.
96) Wang, H.; Xie, H.; Wang, S.; Gao, Z.; Li, C.; Hu, G.-H.; Xiong, C. Enhanced dielectric property and energy storage density of PVDF-HFP based dielectric composites by incorporation of silver nanoparticles-decorated exfoliated montmorillonite nanoplatelets. *Composites Part A: Applied Science and Manufacturing* **2018**, *108*, 62–68, DOI: 10.1016/j.compositesa.2018.02.020, available at https://dx.doi.org/10.1016/j.compositesa.2018.02.020.

97) He, D.; Wang, Y.; Zhang, L.; Song, S.; Deng, Y. Poly(vinylidene fluoride)-Based composites modulated via multiscale two-dimensional fillers for high dielectric performances. *Composites Science and Technology* **2018**, *159*, 162–170, DOI: 10.1016/j.compscitech.2018.02.040, available at https://dx.doi.org/10.1016/j.compscitech.2018.02.040.
98) Wang, F.; Xia, R.; Li, X.; Qin, J.; Shao, H.; Jian, G.; Liu, R.; Wang, F.; Liu, H. Improving the electrical and mechanical performances of embedded capacitance materials by introducing tungsten disulfide nanoflakes into the dielectric layer. *Journal of Materials Science: Materials in Electronics* **2020**, *31* (10), 7889–7897, DOI: 10.1007/s10854-020-03327-5, available at https://dx.doi.org/10.1007/s10854-020-03327-5.
99) Song, S.; Xia, S.; Liu, Y.; Lv, X.; Sun, S. Effect of Na+ MMT-ionic liquid synergy on electroactive, mechanical, dielectric and energy storage properties of transparent PVDF-based nanocomposites. *Chemical Engineering Journal* **2020**, *384*, 123365–123365, DOI: 10.1016/j.cej.2019.123365, available at https://dx.doi.org/10.1016/j.cej.2019.123365.
100) Li, H.; Ren, L.; Ai, D.; Han, Z.; Liu, Y.; Yao, B.; Wang, Q. Ternary polymer nanocomposites with concurrently enhanced dielectric constant and breakdown strength for high-temperature electrostatic capacitors. *InfoMat* **2020**, *2* (2), 389–400, DOI: 10.1002/inf2.12043, available at https://dx.doi.org/10.1002/inf2.12043.
101) Luo, S.; Yu, J.; Yu, S.; Sun, R.; Cao, L.; Liao, W.-H.; Wong, C.-P. Significantly Enhanced Electrostatic Energy Storage Performance of Flexible Polymer Composites by Introducing Highly Insulating-Ferroelectric Microhybrids as Fillers. *Advanced Energy Materials* **2019**, *9* (5), 1803204–1803204, DOI: 10.1002/aenm.201803204, available at https://dx.doi.org/10.1002/aenm.201803204.
102) Lin, Y.; Zhang, Y.; Sun, C.; Zhan, S.; Yuan, Q.; Yang, H. Energy storage performance in polymer dielectrics by introducing 2D SrBi4Ti4O15 nanosheets. *Ceramics International* **2020**, *46* (10), 15270–15275, DOI: 10.1016/j.ceramint.2020.03.066, available at https://dx.doi.org/10.1016/j.ceramint.2020.03.066.
103) Jiang, J.; Shen, Z.; Cai, X.; Qian, J.; Dan, Z.; Lin, Y.; Liu, B.; Nan, C.-W.; Chen, L.; Shen, Y. Polymer Nanocomposites with Interpenetrating Gradient Structure Exhibiting Ultrahigh Discharge Efficiency and Energy Density. *Advanced Energy Materials* **2019**, *9* (15), 1803411–1803411, DOI: 10.1002/aenm.201803411, available at https://dx.doi.org/10.1002/aenm.201803411.
104) Wu, Y.; Wang, Z.; Shen, X.; Liu, X.; Han, N. M.; Zheng, Q.; Mai, Y.-W.; Kim, J.-K. Graphene/Boron Nitride–Polyurethane Microlaminates for Exceptional Dielectric Properties and High Energy Densities. *ACS Applied Materials & Interfaces* **2018**, *10* (31), 26641–26652, DOI: 10.1021/acsami.8b08031, available at https://dx.doi.org/10.1021/acsami.8b08031.
105) Zeng, Y.; Shen, Z.-H.; Shen, Y.; Lin, Y.; Nan, C.-W. High energy density and efficiency achieved in nanocomposite film capacitors via structure modulation. *Applied Physics Letters* **2018**, *112* (10), 103902–103902, DOI: 10.1063/1.5012006, available at https://dx.doi.org/10.1063/1.5012006.
106) Zhu, Y.; Zhu, Y.; Huang, X.; Chen, J.; Li, Q.; He, J.; Jiang, P. High Energy Density Polymer Dielectrics Interlayered by Assembled Boron Nitride Nanosheets. *Advanced Energy Materials* **2019**, *9* (36), 1901826–1901826, DOI: 10.1002/aenm.201901826, available at https://dx.doi.org/10.1002/aenm.201901826.
107) Liu, G.; Zhang, T.; Feng, Y.; Zhang, Y.; Zhang, C.; Zhang, Y.; Wang, X.; Chi, Q.; Chen, Q.; Lei, Q. Sandwich-structured polymers with electrospun boron nitrides layers as high-temperature energy storage dielectrics. *Chemical Engineering Journal* **2020**, *389*, 124443–124443, DOI: 10.1016/j.cej.2020.124443, available at https://dx.doi.org/10.1016/j.cej.2020.124443.